

Nonperturbative study of quantum many-body correlation effects in neutron stars: Equation of state

Hao-Fu Zhu,^{1,2} Xufen Wu,^{1,2} and Guo-Zhu Liu^{3,*}

¹*CAS Key Laboratory for Research in Galaxies and Cosmology, Department of Astronomy, University of Science and Technology of China, Hefei, Anhui 230026, China*

²*School of Astronomy and Space Science, University of Science and Technology of China, Hefei, Anhui 230026, China*

³*Department of Modern Physics, University of Science and Technology of China, Hefei, Anhui 230026, P. R. China*

Although neutron stars have been studied for decades, their internal structure remains enigmatic, mainly due to large uncertainties in the equation of state. In neutron stars, the nucleons are strongly interacting by exchanging mesons, which can lead to significant quantum many-body correlation effects. Mean-field calculations failed to capture these effects. Here, we develop a nonperturbative quantum field-theoretic approach to handle strongly correlated dense nuclear matter within the framework of quantum hadrodynamics. We show that the many-body effects can be incorporated in the Dyson-Schwinger equation of the nucleon propagator. Based on a linear σ - ω - ρ model, we successfully reproduce six empirical observable quantities of saturation nuclear matter by tuning six parameters. After including the many-body effects into the equation of state of realistic neutron star matter, we obtain a mass-radius relation that is comparable with recent astrophysical observations of neutron stars.

I. INTRODUCTION

The physical properties of neutron stars are characterized by a series of observable quantities [1, 2], including the maximal mass, mass-radius (M - R) relation, tidal deformability, moment of inertia, gravitational shift, and so on. Such quantities depend crucially on the equation of state (EOS), which relates the energy density ϵ to the pressure P [3, 4]. Unfortunately, the neutron star EOS has not been determined. Although the internal composition is still in debate, the most common view [1, 2] is that the neutron star core is dominantly composed of neutrons strongly interacting with each other by exchanging various mesons. To ensure causality, it is convenient to use relativistic quantum field theories to describe nucleon-meson (NM) interactions, which defines the framework of quantum hadrodynamics (QHD) [1, 5–22].

According to the extensive investigations of quantum many-particle systems [23], one can affirm that strong NM interactions induce significant quantum correlation effects, such as the Landau damping of nucleon states, the modification of nucleon velocity, and the renormalization of nucleon masses. These effects could markedly change the bulk properties of nuclear matter, and thus should be properly included in the EOS. Unfortunately, such effects are poorly considered in previous works on QHD models. Since the NM interactions are quite strong, ordinary weak perturbation theory is failed. In practice, relativistic mean-field theory (RMFT) has been widely used to study QHD models [1, 5–22]. RMFT has achieved remarkable success in the theoretical description of finite nuclei. However, the nucleon density in the core region of neutron star is much higher than in finite nuclei. As a result, the quantum fluctuation and the correlation effects

are substantially enhanced. RMFT, as a semi-classical method, cannot incorporate such quantum fluctuation and correlation effects. Furthermore, RMFT relies on intricate interactions with many tuning parameters, and often suffers from the instability difficulty [1, 9].

Apart from RMFT, chiral effective field theory (χ EFT) [24, 25] and the quantum Monte Carlo (QMC) method [26] are also frequently applied to study nuclear matter. These two methods can be combined to gain useful constraints on the neutron star EOS [27, 28]. Nevertheless, χ EFT results are reliable only at densities lower than $2\rho_{B0}$, where ρ_{B0} is the nuclear saturation density. Hence, the combination of χ EFT and QMC simulation becomes questionable at high densities [27, 28]. The QMC method also has its limitations. It usually uses a small number of particles in a box to mimic infinite nuclear matter. The validity of this scheme needs to be justified. The QMC simulations also suffer from the fermion sign problem and finite-size effects at high densities.

On the experimental side, astrophysical observations have made significant progress in the past decade. The detection of gravitational waves by the LIGO Scientific and Virgo Collaborations, especially the GW170817 event from the merger of binary neutron stars, has led us to a new era of multimessenger astronomy [29, 30]. The Neutron Star Interior Composition Explorer (NICER) has enabled the simultaneous measurement of the masses and radii of some neutron stars [31–34]. The discovery of several massive neutron stars with masses $> 2.0M_{\odot}$, where M_{\odot} is the solar mass, raised the critical question as to what is the upper limit of neutron star mass [35–38]. These exciting findings provide exceptional opportunities to examine the effects of many-body correlations on the EOS of neutron stars.

In this paper, we propose a nonperturbative quantum field-theoretic approach to handle the strong coupling regime of QHD. This approach surmounts the flaws of weak perturbation and mean-field theories, and is valid

*Corresponding author: gzliu@ustc.edu.cn

within a wide range of nucleon density. We shall show that the effects of many-body correlations can be amply incorporated in the Dyson-Schwinger (DS) equation [39–42] of the renormalized nucleon propagator $G(k)$, where $k \equiv (\varepsilon, \mathbf{k})$ is the four-momentum. After performing a nonperturbative analysis of a linear σ - ω - ρ model that contains six tuning parameters, we acquire a perfect fit to the experimental results of six observable quantities of saturation nuclear matter, including the saturation density ρ_{B0} , binding energy per nucleon E_b , effective nucleon mass m_N^* , compressible modulus K , symmetry energy E_s , and symmetry energy slope L_s .

The simulated model parameters are then adopted to compute the neutron star EOS. In reality, pure neutron matter is not stable [1]. A small fraction of protons, electrons, and muons should be present in neutron star cores. They coexist with neutrons to sustain the β equilibrium as well as the electrical neutrality [1]. The quantum many-body effects caused by the proton-meson interactions can be determined by using our approach. The resulting total EOS of realistic neutron star matter leads to an M - R relation that is dependent on the value of L_s . When L_s is tuned to be roughly $\approx (30 - 50)$ MeV, the radii of low-mass neutron stars produced by our EOS is comparable with astrophysical observations. The corresponding maximal mass of neutron stars is about $2.67 M_\odot$, which, however, might be modified if additional degrees of freedom are considered.

The rest of the paper is organized as follows. In Sec. II, we give the DS equation of the renormalized neutron propagator and decompose it into three self-consistent integral equations. In Sec. III, we derive the expressions of some observable quantities of saturation nuclear matter and compare the results with experiments. In Sec. IV, we obtain the EOS that includes the impact of nonperturbative effects. The results are summarized in Sec. V with a highlight of future research work.

II. DYSON-SCHWINGER EQUATION OF NEUTRON PROPAGATOR

As the first step, we should define an appropriate QHD model as the starting point. The simplest QHD model is the linear σ - ω model, also known as linear Walecka model [5]. Given that perturbation theory is invalid, Walecka employed RMFT to address the linear σ - ω model and reproduced the saturation density ρ_{B0} and the binding energy per nucleon E_b by tuning two Yukawa coupling parameters g_σ and g_ω . However, the RMFT results of other nuclear-matter quantities were at odds with experiments [1]. To remedy this flaw, Bodmer and Bogutta [6] included nonlinear $-b_0\sigma^3$ and $-c_0\sigma^4$ terms to linear σ - ω model. Afterwards, more mesons, such as ρ [7] and δ [8], along with many more free parameters, were introduced to gain a better fitting to the experimental data of nuclear quantities and neutron star observations.

In the past several decades, RMFT has been applied

to study not only finite nuclei but also infinite nuclear matter and neutron stars. Despite such success, RMFT and its variants have obvious limitations [9]. First of all, RMFT is essentially semiclassical as it ignores all the quantum fluctuations of meson fields. In addition, almost all RMFT models contain two nonlinear self-coupling terms of σ mesons: $-b_0\sigma^3$ and $-c_0\sigma^4$. Such terms make a contribution $U(\sigma) = b_0\sigma^3 + c_0\sigma^4$ to the total energy of the system. In many widely used RMFT models, b_0 and/or c_0 take negative values. In that case, the total energy has no lower bound, implying that the systems described by such RMFT models are unstable and would undergo thermodynamic instability once quantum fluctuations become strong enough at high densities. This inconsistency cast serious doubt on the validity of RMFT results. Another problem is that RMFT often needs to manually introduce some intricate interactions. The resultant RMFT models are very complicated, making it difficult to carry out systematic theoretic calculations. These limitations might not be a big problem in finite nuclei where the nucleon density is relatively low. However, quantum fluctuations are greatly enhanced and the nucleon-meson interactions become quite strong in the high-density cores of neutron stars. The quantum many-body effects should be incorporated into the EOS.

We consider a generic σ - ω - ρ - δ QHD model [1, 5]

$$\begin{aligned} \mathcal{L} = & \bar{\psi} (i\partial_\mu \gamma^\mu - m_N) \psi + \frac{1}{2} \partial_\mu \sigma \partial^\mu \sigma - \frac{1}{2} m_\sigma^2 \sigma^2 \\ & - \frac{1}{4} \omega_{\mu\nu} \omega^{\mu\nu} + \frac{1}{2} m_\omega^2 \omega_\mu \omega^\mu \\ & - \frac{1}{4} \rho_{\mu\nu} \cdot \rho^{\mu\nu} + \frac{1}{2} m_\rho^2 \rho_\mu \cdot \rho^\mu \\ & + \frac{1}{2} \partial_\mu \delta \cdot \partial^\mu \delta - \frac{1}{2} m_\delta^2 \delta^2 \\ & + g_\sigma \sigma \bar{\psi} \psi - g_\omega \omega_\mu \bar{\psi} \gamma^\mu \psi \\ & - \frac{1}{2} g_\rho \rho_\mu \cdot \bar{\psi} \boldsymbol{\tau} \gamma^\mu \psi + g_\delta \delta \cdot \bar{\psi} \boldsymbol{\tau} \psi, \end{aligned} \quad (1)$$

where $\partial_\mu = (\partial_t, \boldsymbol{\partial})$. The tensors $\omega_{\mu\nu}$ and $\rho_{\mu\nu}$ are

$$\omega_{\mu\nu} = \partial_\mu \omega_\nu - \partial_\nu \omega_\mu, \quad (2)$$

$$\rho_{\mu\nu} = \partial_\mu \rho_\nu - \partial_\nu \rho_\mu - g_\rho \rho_\mu \times \rho_\nu. \quad (3)$$

The spinor ψ , whose conjugate is $\bar{\psi} = \psi^\dagger \gamma^0$, has eight components for nuclear matter, namely $\psi = (\psi_p, \psi_n)^T$. For a pure neutron matter, $\psi = \psi_n$ has only four components. Nucleons couple to neutral σ mesons, denoted by an isoscalar scalar field σ , neutral vector ω mesons, denoted by an isoscalar vector field ω^μ , charged vector ρ mesons, denoted by an isovector vector field ρ^μ , and charged δ mesons, denoted by an isovector scalar field δ . The Pauli matrices $\boldsymbol{\tau}$ operate in the isospin space. Considering the rotational invariance around the third axis in isospin space, we only retain the isospin three-component of ρ_3^μ and that of δ_3 , namely neutral ρ_0 and neutral δ_0 . The bare nucleon mass is $m_N = 939$ MeV and the rest meson masses are $m_\sigma = 550$ MeV, $m_\omega = 783$ MeV,

$m_\rho = 763$ MeV, and $m_\delta = 980$ MeV. Notice that this model does not contain self-couplings nor cross-couplings of mesons. This avoids the instability difficulty.

At the mean-field level, one replaces the quantum fields σ , ω , ρ , and δ with their mean values $\langle\sigma\rangle$, $\langle\omega\rangle$, $\langle\rho\rangle$, and $\langle\delta\rangle$, respectively. Then the above QHD model can be treated using the standard RMFT procedure [1]. As mentioned at the beginning of this section, such an approximation is not satisfactory. To illustrate the importance of surpassing mean-field theory and developing nonperturbative methods, it is instructive to consider the historical development of the microscopic theory of superconductivity as a reference. While Bardeen-Cooper-Schrieffer (BCS) theory [43] can qualitatively explain the zero resistivity and Meissner effect of superconductivity, the observable quantities, especially the critical temperature T_c , computed based on BCS mean-field theory are unreliable for most materials. To compute observable quantities more precisely, it is necessary to consider some major quantum many-body effects, such as the retardation of phonon propagation and the electron damping, ignored by BCS theory. These effects can be efficiently handled by adopting the nonperturbative Eliashberg theory [44], which treats the electron-phonon interaction in a self-consistent manner and computes T_c by solving a number of nonlinear integral equations. Over the last 60 years, the Eliashberg theory has been the standard microscopic theory of phonon-mediated superconductivity. For many superconductors, the results of T_c obtained by Eliashberg theory are in good agreement with experiments.

Inspired by the great success of Eliashberg theory as a well-justified substitute of BCS mean-field theory, here we employ a nonperturbative approach to handle the strongly correlated dense nuclear matter. Different from RMFT, we view the model of Eq. (1) as a fully fledged quantum field theory and treat the nucleon dynamics and meson dynamics on an equal footing. We find that the nonperturbative effects of QHD models can be taken into account by solving the self-consistent DS equation of nucleon propagator $G(k)$. This sort of approach has been exploited to study dynamical chiral symmetry breaking in particle physics [40] and superconductivity [41] and excitonic insulating transition [42] in condensed matter physics. As far we know, it has not been adopted to compute the EOS and M - R relation of neutron stars.

According to the analysis of the Appendix A, the DS equation of renormalized nucleon propagator $G(k)$ is

$$\begin{aligned} G^{-1}(k) = & G_0^{-1}(k) + ig_\sigma^2 \int \frac{d^4q}{(2\pi)^4} G(k+q) D_0(q) \\ & - ig_\omega^2 \int \frac{d^4q}{(2\pi)^4} \gamma_\mu G(k+q) F_0^{\mu\nu}(q) \gamma_\nu \\ & - i \frac{g_\rho^2}{4} \int \frac{d^4q}{(2\pi)^4} \tau_3 \gamma_\mu G(k+q) V_0^{\mu\nu}(q) \tau_3 \gamma_\nu \\ & - ig_\delta^2 \int \frac{d^4q}{(2\pi)^4} \tau_3 G(k+q) C_0(q) \tau_3. \end{aligned} \quad (4)$$

A schematic Feynman diagram of this equation is shown

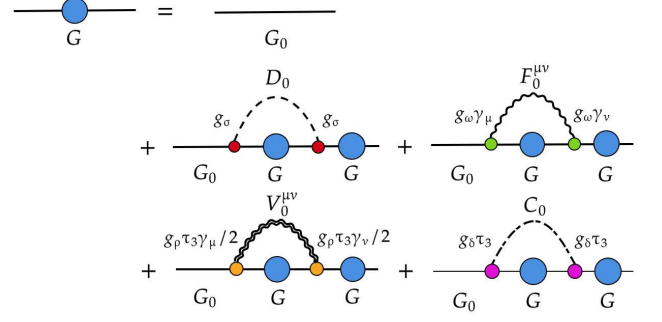


FIG. 1: Diagrammatic illustration of the DS equation of $G(k)$.

in Fig. 1. This DS equation contains, apart from $G(k)$, the free neutron propagator

$$G_0(k) = \frac{1}{k_\mu \gamma^\mu - m_N}, \quad (5)$$

and three free propagators of σ , ω , ρ , and δ_0 mesons:

$$D_0(q) = \frac{1}{q^2 - m_\sigma^2}, \quad (6)$$

$$F_0^{\mu\nu}(q) = -\frac{1}{q^2 - m_\omega^2} \left(g^{\mu\nu} - \frac{q^\mu q^\nu}{m_\omega^2} \right), \quad (7)$$

$$V_0^{\mu\nu}(q) = -\frac{1}{q^2 - m_\rho^2} \left(g^{\mu\nu} - \frac{q^\mu q^\nu}{m_\rho^2} \right), \quad (8)$$

$$C_0(q) = \frac{1}{q^2 - m_\delta^2}. \quad (9)$$

The four-momenta of neutrons and mesons are $k \equiv (\varepsilon, \mathbf{k})$ and $q \equiv (\omega, \mathbf{q})$, respectively. The meson propagators depend on both energy and momentum, so the dynamics of all mesons is incorporated in the DS equation. The values of coupling parameters g_σ , g_ω , g_ρ , and g_δ should be determined by comparing theoretical results with the experimental data of the saturation nuclear matter.

The Fermi energy E_F provides a natural energy scale and can be used to define the integration range of ω . Here, we choose $\omega \in [-\Omega_c, +\Omega_c]$, where $\Omega_c = 1000$ MeV is of the same order of E_F at $6\rho_{B0}$. The absolute value of meson momentum $|\mathbf{q}|$ lies within the range of $[0, \Lambda_c k_F]$, where k_F is the Fermi momentum and Λ_c is a positive tuning parameter. Thus, the integral measure is

$$\int \frac{d^4q}{(2\pi)^4} \equiv \int_{-\Omega_c}^{+\Omega_c} \frac{d\omega}{2\pi} \int_0^{\Lambda_c k_F} \frac{d^3\mathbf{q}}{(2\pi)^3}. \quad (10)$$

All the results are free of divergences, thus it is not necessary to perform renormalization calculations.

As mentioned, our model does not contain self- and cross-coupling terms of the meson fields. However, we still wish to include their potential contributions.

Generic field-theoretic analysis shows that such coupling terms can renormalize meson masses. In light of this, we replace the bare mass m_σ appearing in Eq. (1) and $D_0(q)$ with the renormalized mass m_σ^* and take the ratio m_σ^*/m_σ as an independent tuning parameter. One may let m_ω vary, but tuning m_σ is sufficient.

On generic grounds, one can expand $G(k)$ as

$$G(k) = \frac{1}{A_0(k)\varepsilon\gamma^0 - A_1(k)\mathbf{k} \cdot \boldsymbol{\gamma} - A_2(k)m_N}, \quad (11)$$

where $A_0(k)$, $A_1(k)$, and $A_2(k)$ are the renormalization functions of the wave function (field operator), the neutron velocity, and the neutron mass, respectively. The effects of quantum many-body correlation are embodied in these three functions. In the non-interacting limit, $A_0(k) = A_1(k) = A_2(k) = 1$. The many-body effects are

characterized by the deviation of $A_{0,1,2}(k)$ from unity.

The DS equation is formally very complicated. To simplify calculations, we make some further approximations. On account of the translational invariance and rotational symmetry of infinite nuclear matter, we retain only the contribution of the time component of ω^μ and ρ_3^μ , which is achieved by taking

$$\gamma_\mu \rightarrow \gamma_0, \quad \tau_3 \gamma_\mu \rightarrow \tau_3 \gamma_0, \quad (12)$$

$$F_0^{\mu\nu}(q) \approx F_0^{00}(q), \quad V_0^{\mu\nu}(q) \approx V_0^{00}(q). \quad (13)$$

Moreover, we drop the terms $\frac{q^\mu q^\nu}{m_\omega^2}$ from $F_0^{\mu\nu}(q)$ and $\frac{q^\mu q^\nu}{m_\rho^2}$ from $V_0^{\mu\nu}(q)$ to preserve the baryon number conservation and isospin conservation, respectively. Under such approximations, we substitute the generic propagator (11) into the DS equation (4), and then find

$$\begin{aligned} & A_0(k)\varepsilon\gamma^0 - A_1(k)\mathbf{k} \cdot \boldsymbol{\gamma} - A_2(k)m_N - \varepsilon\gamma^0 + \mathbf{k} \cdot \boldsymbol{\gamma} + m_N \\ = & -ig_\sigma^2 \int \frac{d^4q}{(2\pi)^4} \frac{1}{A_0(k+q)(\varepsilon+\omega)\gamma^0 - A_1(k+q)(\mathbf{k}+\mathbf{q}) \cdot \boldsymbol{\gamma} - A_2(k+q)m_N} D_0(q) \\ & -ig_\omega^2 \int \frac{d^4q}{(2\pi)^4} \gamma^0 \frac{1}{A_0(k+q)(\varepsilon+\omega)\gamma^0 - A_1(k+q)(\mathbf{k}+\mathbf{q}) \cdot \boldsymbol{\gamma} - A_2(k+q)m_N} F_0^{00}(q)\gamma_0 \\ & -i\frac{g_\rho^2}{4} \int \frac{d^4q}{(2\pi)^4} \tau_3 \gamma_0 \frac{1}{A_0(k+q)(\varepsilon+\omega)\gamma^0 - A_1(k+q)(\mathbf{k}+\mathbf{q}) \cdot \boldsymbol{\gamma} - A_2(k+q)m_N} V_0^{00}(q)\tau_3 \gamma_0 \\ & -ig_\delta^2 \int \frac{d^4q}{(2\pi)^4} \tau_3 \frac{1}{A_0(k+q)(\varepsilon+\omega)\gamma^0 - A_1(k+q)(\mathbf{k}+\mathbf{q}) \cdot \boldsymbol{\gamma} - A_2(k+q)m_N} C_0(q)\tau_3. \end{aligned} \quad (14)$$

This single equation can be decomposed into three integral equations. For instance, multiplying γ^0 and $\boldsymbol{\gamma}$ to both sides of Eq. (14) and then calculating the trace, one would get the equations for $A_0(k)$ and $A_1(k)$, respectively. Computing the trace of both sides of Eq. (14) yields the equation of $A_2(k)$. These three equations are nonlinear and coupled to each other. Solving them requires enormous computational resources. The computational time can be substantially reduced if these equations have only one integration variable. One could ignore either the momentum dependence or the energy dependence of $A_0(k)$, $A_1(k)$, and $A_2(k)$. According to our numerical calculations, $A_0(k)$, $A_1(k)$, and $A_2(k)$ exhibit a rather weak dependence on the momentum \mathbf{k} for a fixed energy. It is therefore justified to fix their \mathbf{k} at Fermi momentum \mathbf{k}_F and set $A_{0,1,2}(\varepsilon, \mathbf{k}_F) \equiv A_{0,1,2}(\varepsilon)$. We emphasize here that this approximation does not entirely neglect the momentum dependence. In particular, the Fermi surface is still present and Pauli's exclusion principle continues to play an essential role. The nonlinear integral equations of $A_0(\varepsilon)$, $A_1(\varepsilon)$, and $A_2(\varepsilon)$ are

$$\begin{aligned} A_0(\varepsilon) = & 1 - \frac{i}{\varepsilon} \int \frac{d\omega d^3\mathbf{q}}{(2\pi)^4} \frac{A_0(\varepsilon+\omega)(\varepsilon+\omega)}{A_0^2(\varepsilon+\omega)(\varepsilon+\omega)^2 - A_1^2(\varepsilon+\omega)(\mathbf{k}+\mathbf{q})^2 - A_2^2(\varepsilon+\omega)m_N^2} \\ & \times \left(\frac{g_\sigma^2}{\omega^2 - \mathbf{q}^2 - m_\sigma^2} - \frac{g_\omega^2}{\omega^2 - \mathbf{q}^2 - m_\omega^2} - \frac{g_\rho^2/4}{\omega^2 - \mathbf{q}^2 - m_\rho^2} + \frac{g_\delta^2}{\omega^2 - \mathbf{q}^2 - m_\delta^2} \right), \end{aligned} \quad (15)$$

$$\begin{aligned} A_1(\varepsilon) = & 1 - \frac{i}{|\mathbf{k}|} \int \frac{d\omega d^3\mathbf{q}}{(2\pi)^4} \frac{A_1(\varepsilon+\omega)|\mathbf{k}+\mathbf{q}|}{A_0^2(\varepsilon+\omega)(\varepsilon+\omega)^2 - A_1^2(\varepsilon+\omega)(\mathbf{k}+\mathbf{q})^2 - A_2^2(\varepsilon+\omega)m_N^2} \\ & \times \left(\frac{g_\sigma^2}{\omega^2 - \mathbf{q}^2 - m_\sigma^2} + \frac{g_\omega^2}{\omega^2 - \mathbf{q}^2 - m_\omega^2} + \frac{g_\rho^2/4}{\omega^2 - \mathbf{q}^2 - m_\rho^2} + \frac{g_\delta^2}{\omega^2 - \mathbf{q}^2 - m_\delta^2} \right), \end{aligned} \quad (16)$$

$$\begin{aligned} A_2(\varepsilon) = & 1 + \frac{i}{m_N} \int \frac{d\omega d^3\mathbf{q}}{(2\pi)^4} \frac{A_2(\varepsilon+\omega)m_N}{A_0^2(\varepsilon+\omega)(\varepsilon+\omega)^2 - A_1^2(\varepsilon+\omega)(\mathbf{k}+\mathbf{q})^2 - A_2^2(\varepsilon+\omega)m_N^2} \\ & \times \left(\frac{g_\sigma^2}{\omega^2 - \mathbf{q}^2 - m_\sigma^2} - \frac{g_\omega^2}{\omega^2 - \mathbf{q}^2 - m_\omega^2} - \frac{g_\rho^2/4}{\omega^2 - \mathbf{q}^2 - m_\rho^2} + \frac{g_\delta^2}{\omega^2 - \mathbf{q}^2 - m_\delta^2} \right). \end{aligned} \quad (17)$$

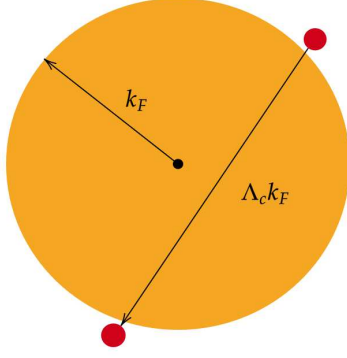


FIG. 2: A nucleon staying on the Fermi surface is scattered by mesons into another point.

The integration range for variable $|\mathbf{q}|$ is $|\mathbf{q}| \in [0, \Lambda_c k_F]$, where k_F is the Fermi momentum and Λ_c is a positive constant. For a nucleon located precisely on the Fermi surface, it is scattered by mesons into a different point on the surface. In principle, the maximal value of the transferred momentum is $|\mathbf{q}|_{\max} = 2k_F$. Please see Fig. 2 for a schematic illustration. However, the scattering process with large momenta could be considerably suppressed by

such heavy intermediate mesons as ω , ρ , and δ . Thus, the actual upper limit of $|\mathbf{q}|$ may take some different value from $2k_F$. It is therefore more convenient to take the upper cutoff to be $|\mathbf{q}|_{\max} = \Lambda_c k_F$, where Λ_c serves as an independent tuning parameter. The integration range for energy ω is $[-\Omega_c, \Omega_c]$. To include more scattering processes, Ω_c should be sufficiently large. Suppose that the nucleon density is as high as $6\rho_{B0}$ in the center of neutron star core, then the Fermi energy would be roughly $E_F = \sqrt{k_F^2 + m_N^2} \approx 1000$ MeV. Thus, here we choose to take $\Omega_c = 1000$ MeV, which appears to be large enough. One could adopt a different value, say $\Omega_c = 1500$ MeV. Then, all the tuning parameters would take slightly different values, which eventually leads to only a minor change to the final EOS of neutron stars.

To facilitate numerical computations, we re-define the internal energy as $\omega \rightarrow \omega - \varepsilon$ and the momentum as $\mathbf{q} \rightarrow \mathbf{q} - \mathbf{k}$, and also introduce Matsubara energy $\varepsilon \rightarrow i\varepsilon$ and $\omega \rightarrow i\omega$. In spherical coordinates, with \mathbf{q} direction being the axis, we have $k_x = |\mathbf{k}|$, and $k_y = k_z = 0$. Accordingly,

$$q_x = |\mathbf{q}| \sin \theta \cos \varphi, \quad q_y = |\mathbf{q}| \sin \theta \sin \varphi, \quad q_z = |\mathbf{q}| \cos \theta. \quad (18)$$

Then the above integral equations become

$$\begin{aligned} A_0(\varepsilon) &= 1 + \frac{1}{\varepsilon} \int \frac{d\omega |\mathbf{q}|^2 d|\mathbf{q}| d\cos\theta d\varphi}{(2\pi)^4} \frac{A_0(\omega)\omega}{A_0^2(\omega)\omega^2 + A_1^2(\omega)|\mathbf{q}|^2 + A_2^2(\omega)m_N^2} \\ &\quad \times \left(\frac{g_\sigma^2}{(\omega - \varepsilon)^2 + |\mathbf{q}|^2 - 2|\mathbf{q}||\mathbf{k}| \sin\theta \cos\varphi + |\mathbf{k}|^2 + m_\sigma^2} - \frac{g_\omega^2}{(\omega - \varepsilon)^2 + |\mathbf{q}|^2 - 2|\mathbf{q}||\mathbf{k}| \sin\theta \cos\varphi + |\mathbf{k}|^2 + m_\omega^2} \right. \\ &\quad \left. - \frac{g_\rho^2/4}{(\omega - \varepsilon)^2 + |\mathbf{q}|^2 - 2|\mathbf{q}||\mathbf{k}| \sin\theta \cos\varphi + |\mathbf{k}|^2 + m_\rho^2} + \frac{g_\delta^2}{(\omega - \varepsilon)^2 + |\mathbf{q}|^2 - 2|\mathbf{q}||\mathbf{k}| \sin\theta \cos\varphi + |\mathbf{k}|^2 + m_\delta^2} \right), \\ A_1(\varepsilon) &= 1 + \frac{1}{|\mathbf{k}|} \int \frac{d\omega |\mathbf{q}|^2 d|\mathbf{q}| d\cos\theta d\varphi}{(2\pi)^4} \frac{A_1(\omega)|\mathbf{q}| \sin\theta \cos\varphi}{A_0^2(\omega)\omega^2 + A_1^2(\omega)|\mathbf{q}|^2 + A_2^2(\omega)m_N^2} \\ &\quad \times \left(\frac{g_\sigma^2}{(\omega - \varepsilon)^2 + |\mathbf{q}|^2 - 2|\mathbf{q}||\mathbf{k}| \sin\theta \cos\varphi + |\mathbf{k}|^2 + m_\sigma^2} + \frac{g_\omega^2}{(\omega - \varepsilon)^2 + |\mathbf{q}|^2 - 2|\mathbf{q}||\mathbf{k}| \sin\theta \cos\varphi + |\mathbf{k}|^2 + m_\omega^2} \right. \\ &\quad \left. + \frac{g_\rho^2/4}{(\omega - \varepsilon)^2 + |\mathbf{q}|^2 - 2|\mathbf{q}||\mathbf{k}| \sin\theta \cos\varphi + |\mathbf{k}|^2 + m_\rho^2} + \frac{g_\delta^2}{(\omega - \varepsilon)^2 + |\mathbf{q}|^2 - 2|\mathbf{q}||\mathbf{k}| \sin\theta \cos\varphi + |\mathbf{k}|^2 + m_\delta^2} \right), \\ A_2(\varepsilon) &= 1 - \frac{1}{m_N} \int \frac{d\omega |\mathbf{q}|^2 d|\mathbf{q}| d\cos\theta d\varphi}{(2\pi)^4} \frac{A_2(\omega)m_N}{A_0^2(\omega)\omega^2 + A_1^2(\omega)|\mathbf{q}|^2 + A_2^2(\omega)m_N^2} \\ &\quad \times \left(\frac{g_\sigma^2}{(\omega - \varepsilon)^2 + |\mathbf{q}|^2 - 2|\mathbf{q}||\mathbf{k}| \sin\theta \cos\varphi + |\mathbf{k}|^2 + m_\sigma^2} - \frac{g_\omega^2}{(\omega - \varepsilon)^2 + |\mathbf{q}|^2 - 2|\mathbf{q}||\mathbf{k}| \sin\theta \cos\varphi + |\mathbf{k}|^2 + m_\omega^2} \right. \\ &\quad \left. - \frac{g_\rho^2/4}{(\omega - \varepsilon)^2 + |\mathbf{q}|^2 - 2|\mathbf{q}||\mathbf{k}| \sin\theta \cos\varphi + |\mathbf{k}|^2 + m_\rho^2} + \frac{g_\delta^2}{(\omega - \varepsilon)^2 + |\mathbf{q}|^2 - 2|\mathbf{q}||\mathbf{k}| \sin\theta \cos\varphi + |\mathbf{k}|^2 + m_\delta^2} \right). \end{aligned}$$

For calculational convenience, it is useful to divide all the

energy and momenta by $\Lambda_c k_F$. $|\mathbf{q}|$ becomes a dimension-

less variable after it is re-scaled as

$$|\mathbf{q}| \rightarrow \frac{|\mathbf{q}|}{\Lambda_c k_F}. \quad (19)$$

The re-scaled dimensionless variable $|\mathbf{q}|$ is defined in the range $|\mathbf{q}| \in [0, 1]$. The re-scaled energy is defined in the range $\omega \in \left[-\frac{\Omega_c}{\Lambda_c k_F}, \frac{\Omega_c}{\Lambda_c k_F}\right]$.

These integral equations are self-consistent and should be solved by using suitable numerical techniques. We will solve them by means of iteration method [41]. First, let $A_{0,1,2}$ take some initial values, which might be $A_0 = A_1 = A_2 = 1$. Second, substitute the initial values into the equations of $A_{0,1,2}$ to obtain a set of new values of $A_{0,1,2}$, which are normally different from initial values. Third, insert these new values again into the equations of $A_{0,1,2}$ to obtain another set of new values of $A_{0,1,2}$. After i times of iteration, one obtains A_0^i , A_1^i , and A_2^i , which are then substituted into the coupled equations to get A_0^{i+1} , A_1^{i+1} , and A_2^{i+1} . Repeat such an operation many times until the difference between i results and $(i+1)$ results vanishes. The error factors created after i iterations are

$$\text{EPS}_{0,1,2}(i) = \frac{1}{N} \sum_{n=1}^N \frac{|A_{0,1,2}^i(n) - A_{0,1,2}^{i-1}(n)|}{|A_{0,1,2}^i(n)| + |A_{0,1,2}^{i-1}(n)|}. \quad (20)$$

For a given nucleon density ρ_B^* , $\text{EPS}_{0,1,2}(i)$ are found to decrease gradually with increasing i . Once $\text{EPS}_{0,1,2}(i)$ become sufficiently small, the iteration process can be terminated. Then the final results of A_0 , A_1 , and A_2 are determined. In realistic calculations, convergence is believed to be achieved once $\text{EPS}_{0,1,2} < 10^{-6}$. Such convergent solutions of $A_{0,1,2}(\varepsilon)$ lead to the renormalized neutron propagator $G(k)$.

III. EQUATION OF STATES OF NEUTRON STAR MATTER

Our next step is to incorporate quantum many-body effects into the EOS of neutron star. In principle, one could first calculate the Luttinger-Ward (LW) functional [45] based on the renormalized neutron propagator $G(k)$ obtained from solving the DS equation and then use this functional to determine the EOS. Such calculations are technically quite involved. Below, we will compute the EOS by taking a route that is less rigorous but more practicable.

Within the framework of RMFT [1], the analytical expressions of the energy density ϵ and the pressure P can be derived. This is a noticeable advantage of RMFT. We wish to obtain the analytical expressions of ϵ and P after including the many-body effects. We find that this goal can be achieved by performing RMFT calculations based

on the following renormalized Lagrangian density

$$\begin{aligned} \mathcal{L}_R = & \bar{\psi}(i\bar{A}_0\partial_t\gamma^0 + i\bar{A}_1\boldsymbol{\partial} \cdot \boldsymbol{\gamma} - \bar{A}_2m_N)\psi \\ & + \frac{1}{2}\partial_\mu\sigma\partial^\mu\sigma - \frac{1}{2}m_\sigma^2\sigma^2 \\ & - \frac{1}{4}\omega_{\mu\nu}\omega^{\mu\nu} + \frac{1}{2}m_\omega^2\omega_\mu\omega^\mu \\ & - \frac{1}{4}\boldsymbol{\rho}_{\mu\nu} \cdot \boldsymbol{\rho}^{\mu\nu} + \frac{1}{2}m_\rho^2\boldsymbol{\rho}_\mu \cdot \boldsymbol{\rho}^\mu \\ & + \frac{1}{2}\partial_\mu\boldsymbol{\delta} \cdot \partial^\mu\boldsymbol{\delta} - \frac{1}{2}m_\delta^2\boldsymbol{\delta}^2 \\ & + g_\sigma\sigma\bar{\psi}\psi - g_\omega\omega_\mu\bar{\psi}\gamma^\mu\psi \\ & - \frac{1}{2}g_\rho\boldsymbol{\rho}_\mu \cdot \bar{\psi}\boldsymbol{\tau}\gamma^\mu\psi + g_\delta\boldsymbol{\delta} \cdot \bar{\psi}\boldsymbol{\tau}\psi. \end{aligned} \quad (21)$$

This Lagrangian density is written down based on the assumption that the many-body effects are included in three constants $\bar{A}_{0,1,2}$ that are averaged as follows

$$\bar{A}_{0,1,2} = \frac{\int \bar{A}_{0,1,2}(\varepsilon)d\varepsilon}{\int d\varepsilon}. \quad (22)$$

Although these three constants are density dependent, we assume that $\bar{A}_{0,1,2}$ are density independent near the saturation density. This approximation makes it much easier to perform the partial derivative $\frac{\partial}{\partial\rho_B^*}$, and allows us to eventually obtain the analytical expressions of the EOS and observable nuclear quantities. Later, we will discuss the validity of this approximation.

We then apply the standard RMFT [1] to deal with \mathcal{L}_R . From Eq. (21), it is easy to get the equation of motion of the nucleon field

$$\begin{aligned} & [i\bar{A}_0\partial_t\gamma^0 + i\bar{A}_1\boldsymbol{\partial} \cdot \boldsymbol{\gamma} - \bar{A}_2m_N]\psi(z) \\ & = -g_\sigma\sigma(z)\psi(z) + g_\omega\omega_\mu(z)\gamma^\mu\psi(z) \\ & + \frac{g_\rho}{2}\boldsymbol{\rho}_\mu(z) \cdot \boldsymbol{\tau}\gamma^\mu\psi(z) - g_\delta\boldsymbol{\delta}(z) \cdot \boldsymbol{\tau}\psi(z). \end{aligned} \quad (23)$$

The equations of motion of the meson fields are

$$(\partial_\mu\partial^\mu + m_\sigma^2)\sigma(z) = g_\sigma\bar{\psi}(z)\psi(z), \quad (24)$$

$$\partial_\mu\omega^{\mu\nu}(z) + m_\omega^2\omega^\nu(z) = g_\omega\bar{\psi}(z)\gamma^\nu\psi(z), \quad (25)$$

$$\begin{aligned} \partial_\mu\boldsymbol{\rho}^{\mu\nu}(z) + m_\rho^2\boldsymbol{\rho}^\nu(z) &= \frac{g_\rho}{2}\bar{\psi}(z)\boldsymbol{\tau}\gamma^\nu\psi(z) \\ &+ g_\rho\boldsymbol{\rho}_\mu(z) \times \boldsymbol{\rho}^{\mu\nu}(z), \end{aligned} \quad (26)$$

$$(\partial_\mu\partial^\mu + m_\delta^2)\boldsymbol{\delta}(z) = g_\delta\bar{\psi}(z)\boldsymbol{\tau}\psi(z). \quad (27)$$

At mean-field level, all the meson fields are substituted by their mean values, namely

$$\sigma(z) \rightarrow \langle\sigma(z)\rangle = \sigma, \quad (28)$$

$$\omega_\mu(z) \rightarrow \langle\omega_\mu(z)\rangle = \omega_0, \quad (29)$$

$$\boldsymbol{\rho}_\mu(z) \rightarrow \langle\boldsymbol{\rho}_\mu(z)\rangle = \rho_{0(3)}, \quad (30)$$

$$\boldsymbol{\delta}(z) \rightarrow \langle\boldsymbol{\delta}(z)\rangle = \delta_3. \quad (31)$$

Then the renormalized Lagrangian density given by

Eq. (21) becomes

$$\begin{aligned}\mathcal{L}_R^{\text{MF}} = & \bar{\psi}(z)(i\bar{A}_0\partial_t\gamma^0 + i\bar{A}_1\boldsymbol{\partial}\cdot\boldsymbol{\gamma} - \bar{A}_2m_N)\psi(z) \\ & - \frac{1}{2}m_\sigma^2\sigma^2 + \frac{1}{2}m_\omega^2\omega_0^2 + \frac{1}{2}m_\rho^2\rho_{0(3)}^2 - \frac{1}{2}m_\delta^2\delta_3^2 \\ & + g_\sigma\sigma\bar{\psi}(z)\psi(z) - g_\omega\omega_0\bar{\psi}(z)\gamma^0\psi(z) \\ & - \frac{g_\rho}{2}\rho_{0(3)}\bar{\psi}(z)\tau_3\gamma^0\psi(z) \\ & + g_\delta\delta_3\bar{\psi}(z)\tau_3\psi(z).\end{aligned}\quad (32)$$

Then Eq. (23) is simplified to

$$\begin{aligned}& [i\bar{A}_0\partial_t\gamma^0 + i\bar{A}_1\boldsymbol{\partial}\cdot\boldsymbol{\gamma} - g_\omega\omega_0\gamma^0 - \frac{g_\rho}{2}\rho_{0(3)}\tau_3\gamma^0 \\ & - (\bar{A}_2m_N - g_\sigma\sigma - g_\delta\delta_3\tau_3)]\psi(z) = 0,\end{aligned}\quad (33)$$

and Eqs. (24)-(27) are converted to

$$\begin{aligned}\sigma &= \frac{g_\sigma}{m_\sigma^2}\langle\bar{\psi}(z)\psi(z)\rangle \\ &= \frac{g_\sigma}{m_\sigma^{*2}}\rho_s^*,\end{aligned}\quad (34)$$

$$\begin{aligned}\omega^0 &= \frac{g_\omega}{m_\omega^2}\langle\bar{\psi}(z)\gamma^0\psi(z)\rangle = \frac{g_\omega}{m_\omega^2}\langle\psi^\dagger(z)\psi(z)\rangle \\ &= \frac{g_\omega}{m_\omega^2}\rho_B^*,\end{aligned}\quad (35)$$

$$\begin{aligned}\rho_3^0 &= \frac{g_\rho}{2m_\rho^2}\langle\bar{\psi}(z)\tau_3\gamma^0\psi(z)\rangle = \frac{g_\rho}{2m_\rho^2}\langle\psi^\dagger(z)\tau_3\psi(z)\rangle \\ &= \frac{g_\rho}{2m_\rho^2}\rho_3^*,\end{aligned}\quad (36)$$

$$\begin{aligned}\delta_3 &= \frac{g_\delta}{m_\delta^2}\langle\bar{\psi}(z)\tau_3\psi(z)\rangle \\ &= \frac{g_\delta}{m_\delta^2}\rho_{s3}^*.\end{aligned}\quad (37)$$

Here, a raised asterisk is used to denote the inclusion of quantum many-body effects. The baryon density is $\rho_B^* = \rho_p^* + \rho_n^*$, where

$$\rho_i^* = 2 \int_0^{k_{F,i}} \frac{d^3\mathbf{k}}{(2\pi)^3} \frac{1}{\bar{A}_{0,i}} \quad (38)$$

is the renormalized baryon density. The renormalized scalar density is $\rho_s^* = \rho_{s,p}^* + \rho_{s,n}^*$, where

$$\rho_{s,i}^* = 2 \int_0^{k_{F,i}} \frac{d^3\mathbf{k}}{(2\pi)^3} \frac{m_N^*/\bar{A}_{0,i}}{E_{F,i}^*(\mathbf{k})}, \quad (39)$$

$$E_{F,i}^*(\mathbf{k}) = \sqrt{\frac{\bar{A}_{1,i}^2}{\bar{A}_{0,i}^2}\mathbf{k}^2 + m_{N,i}^{*2}}, \quad (40)$$

$$m_{N,i}^* = \frac{\bar{A}_{2,i}m_{N,i} - \frac{g_\sigma^2}{m_\sigma^{*2}}\rho_s^* - \frac{g_\delta^2}{m_\delta^2}\rho_{s3}^*\tau_3}{\bar{A}_{0,i}}, \quad (41)$$

and we have replaced m_σ with the renormalized σ meson mass m_σ^* . The renormalized isospin density is

$$\rho_3^* = \rho_p^* - \rho_n^* = (2y - 1)\rho_B^*, \quad (42)$$

where the proton fraction is $y = \rho_p^*/\rho_B^*$. The renormalized isospin scalar density is

$$\rho_{s3}^* = \rho_{s,p}^* - \rho_{s,n}^*. \quad (43)$$

It is emphasized that the above results are applicable to both symmetric and asymmetric nuclear matter. The fraction of neutrons can be easily tuned by changing the value of y .

A. EOS and observable quantities

The expectation value of the energy-momentum tensor in the rest frame of the matter is diagonal, namely

$$\langle T^{\mu\nu} \rangle = \text{diag}(\epsilon, P, P, P). \quad (44)$$

Then the energy density $\epsilon = \langle T^{00} \rangle$ and the pressure $P = \frac{1}{3}\langle T^{ii} \rangle$ of the system are given by

$$\begin{aligned}\epsilon &= \sum_{i=p,n} 2 \int_0^{k_{F,i}} \frac{d^3\mathbf{k}}{(2\pi)^3} E_{F,i}^*(\mathbf{k}) + \frac{g_\sigma^2}{2m_\sigma^{*2}}\rho_s^{*2} + \frac{g_\omega^2}{2m_\omega^2}\rho_B^{*2} \\ &+ \frac{g_\rho^2}{8m_\rho^2}\rho_3^{*2} + \frac{g_\delta^2}{2m_\delta^2}\rho_{s3}^{*2},\end{aligned}\quad (45)$$

$$\begin{aligned}P &= \sum_{i=p,n} \frac{2}{3} \int_0^{k_{F,i}} \frac{d^3\mathbf{k}}{(2\pi)^3} \frac{\bar{A}_{1,i}\mathbf{k}^2/\bar{A}_{0,i}^2}{E_{F,i}^*(\mathbf{k})} - \frac{g_\sigma^2}{2m_\sigma^{*2}}\rho_s^{*2} \\ &+ \frac{g_\omega^2}{2m_\omega^2}\rho_B^{*2} + \frac{g_\rho^2}{8m_\rho^2}\rho_3^{*2} - \frac{g_\delta^2}{2m_\delta^2}\rho_{s3}^{*2}.\end{aligned}\quad (46)$$

We have verified that the thermodynamic relationship $P = \rho_B^{*2} \frac{\partial(\epsilon/\rho_B^*)}{\partial\rho_B^*}$ is satisfied. The above expressions of ϵ and P are then used to compute the binding energy E_b , the effective nucleon mass m_N^* , the compressible modulus K , and the symmetry energy E_s at the saturation density of symmetric nuclear matter as follows

$$E_b = \frac{\epsilon}{\rho_B^*} - m_N, \quad (47)$$

$$m_N^* = \frac{\bar{A}_2m_N - \frac{g_\sigma^2}{m_\sigma^{*2}}\rho_s^*}{\bar{A}_0}, \quad (48)$$

$$\begin{aligned}K &= 9\rho_B^{*2} \frac{\partial^2(\epsilon/\rho_B^*)}{\partial\rho_B^{*2}} \\ &= \frac{3\bar{A}_1^2k_F^2}{E_F^*} + \frac{9g_\omega^2\rho_B^*}{m_\omega^2} - \frac{9g_\sigma^2\frac{m_N^{*2}}{E_F^*}\rho_B^*}{m_\sigma^{*2} + \frac{3g_\delta^2}{\bar{A}_0}(\frac{\rho_s^*}{m_N^*} - \frac{\rho_B^*}{E_F^*})}\end{aligned}\quad (49)$$

$$\begin{aligned}E_s &= \frac{1}{8} \frac{\partial^2(\epsilon/\rho_B^*)}{\partial y^2} \\ &= \frac{\bar{A}_1^2k_F^2}{6E_F^*} + \frac{g_\rho^2\rho_B^*}{8m_\rho^2} - \frac{g_\delta^2\frac{m_N^{*2}}{2E_F^{*2}}\rho_B^*}{m_\delta^2 + \frac{3g_\delta^2}{\bar{A}_0}(\frac{\rho_s^*}{m_N^*} - \frac{\rho_B^*}{E_F^*})}.\end{aligned}\quad (50)$$

The symmetry energy slope L_s is found to have the following complicated analytical expression:

$$\begin{aligned}
L_s &= 3\rho_B^* \frac{\partial E_s}{\partial \rho_B^*} \\
&= \frac{\bar{A}_1^2 k_F^2}{3E_F^*} + \frac{3g_\rho^2 \rho_B^*}{8m_\rho^2} - \frac{\bar{A}_1^4 k_F^4}{6E_F^{*3}} \left(1 - \frac{\frac{g_\sigma^2}{\bar{A}_1^2} \frac{2m_N^{*2}}{\pi^2 E_F^*} k_F}{m_\sigma^{*2} + \frac{3g_\sigma^2}{\bar{A}_0} \left(\frac{\rho_s^*}{m_N^*} - \frac{\rho_B^*}{E_F^*} \right)} \right) \\
&\quad - \frac{g_\delta^2 \frac{m_N^{*2}}{2E_F^{*2}} \rho_B^*}{m_\delta^2 + \frac{3g_\delta^2}{\bar{A}_0} \left(\frac{\rho_s^*}{m_N^*} - \frac{\rho_B^*}{E_F^*} \right)} \left\{ 3 - \frac{2\bar{A}_1^2 k_F^2}{E_F^{*2}} - \frac{6\frac{g_\sigma^2}{\bar{A}_0} \left(\frac{1}{E_F^*} - \frac{m_N^{*2}}{E_F^{*3}} \right) \rho_B^*}{m_\sigma^{*2} + \frac{3g_\sigma^2}{\bar{A}_0} \left(\frac{\rho_s^*}{m_N^*} - \frac{\rho_B^*}{E_F^*} \right)} + \frac{3g_\delta^2 \rho_B^*}{m_\delta^2 + \frac{3g_\delta^2}{\bar{A}_0} \left(\frac{\rho_s^*}{m_N^*} - \frac{\rho_B^*}{E_F^*} \right)} \right. \\
&\quad \times \left. \left[\frac{6\frac{g_\sigma^2}{\bar{A}_0^2} \frac{1}{E_F^*} \left(\frac{\rho_s^*}{m_N^*} - \frac{\rho_B^*}{E_F^*} \right)}{m_\sigma^{*2} + \frac{3g_\sigma^2}{\bar{A}_0} \left(\frac{\rho_s^*}{m_N^*} - \frac{\rho_B^*}{E_F^*} \right)} - \frac{\bar{A}_1^2 k_F^2}{E_F^{*3}} \left(1 + \frac{3\frac{g_\sigma^2}{\bar{A}_0} \frac{\rho_B^*}{E_F^*}}{m_\sigma^{*2} + \frac{3g_\sigma^2}{\bar{A}_0} \left(\frac{\rho_s^*}{m_N^*} - \frac{\rho_B^*}{E_F^*} \right)} \right) \right] \right\}. \tag{51}
\end{aligned}$$

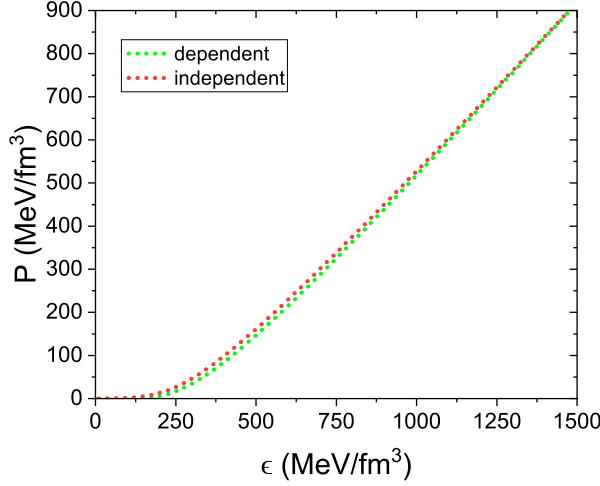


FIG. 3: Comparing the EOS of a pure neutron matter generated by including the density dependence of $\bar{A}_{0,1,2}$ to the one obtained by ignoring the density dependence of $\bar{A}_{0,1,2}$.

The theoretical results ρ_{B0} , E_b , m_N^* , K , E_s , and L_s depend on tuning parameters g_σ , g_ω , g_ρ , g_δ , m_σ^*/m_σ , and Λ_c . We require such tuning parameters to take all the possible values, exploiting the Markov chain Monte Carlo [46] method, until the theoretical results of these quantities are compatible with the experimental data: $\rho_{B0} = (0.16 \pm 0.01) \text{ fm}^{-3}$, $E_b = (-16 \pm 1) \text{ MeV}$, $m_N^*/m_N = (0.56 - 0.75)$, $K = (240 \pm 20) \text{ MeV}$, $E_s = (28 - 34) \text{ MeV}$, and $L_s = (40 - 68) \text{ MeV}$.

By adjusting g_σ , g_ω and g_ρ , previous RMFT studies of the σ - ω - ρ model [1] have yielded $\rho_{B0} = 0.153 \text{ fm}^{-3}$, $E_b = -16.3 \text{ MeV}$, $m_N^*/m_N = 0.50$, $K = 550 \text{ MeV}$, and $E_s = 32.5 \text{ MeV}$. Apparently, m_N^* is too small and K is too large. To obtain larger m_N^* and smaller K , it is necessary to introduce more tuning parameters. In RMFT, this problem is solved by manually including some nonlinear meson coupling terms, such as $-b_0\sigma^3$, $-c_0\sigma^4$, and $-d_0\sigma^2\omega^2$. As mentioned in Sec. I, such nonlinear terms

might drive the system to become unstable. We find it sufficient to tune one single parameter: the ratio m_σ^*/m_σ .

The above analytical results were obtained by ignoring the density dependence of $\bar{A}_{0,1,2}$. It is straightforward to take into account the density dependence of $\bar{A}_{0,1,2}$. But then it becomes impossible to derive the analytical expressions of these quantities. We performed direct numerical calculations based on density dependent $\bar{A}_{0,1,2}$ and show the results in Fig. 3. One can see that the inclusion of the density dependence of $\bar{A}_{0,1,2}$ only slightly modifies the final EOS. Therefore, it is well justified to drop the density dependence of $\bar{A}_{0,1,2}$ in the calculation of the above observable quantities.

B. β equilibrium

While a pure neutron matter fulfils the charge neutrality requirement, it cannot be stable. In the cores of neutron stars, there are also, in addition to neutrons, a small fraction of protons and electrons. As the density ρ_B^* increases, some electrons are replaced by muons when the Fermi energy of electrons surpasses the rest energy of muons, which is energetically more favorable. The conditions of chemical equilibrium [1] are

$$\mu_p + \mu_e = \mu_n, \tag{52}$$

$$\mu_e = \mu_\mu, \tag{53}$$

where the chemical potentials of neutrons, protons, electrons, and muons are given by

$$\mu_n = \sqrt{\frac{\bar{A}_{1,n}^2}{\bar{A}_{0,n}^2} k_n^2 + m_{N,n}^{*2}} + \frac{g_\omega^2}{m_\omega^2} \rho_B^* - \frac{g_\rho^2}{4m_\rho^2} \rho_3^*, \tag{54}$$

$$\mu_p = \sqrt{\frac{\bar{A}_{1,p}^2}{\bar{A}_{0,p}^2} k_p^2 + m_{N,p}^{*2}} + \frac{g_\omega^2}{m_\omega^2} \rho_B^* + \frac{g_\rho^2}{4m_\rho^2} \rho_3^*, \tag{55}$$

$$\mu_e = \sqrt{k_e^2 + m_e^2}, \tag{56}$$

$$\mu_\mu = \sqrt{k_\mu^2 + m_\mu^2}. \tag{57}$$

Here, k_n , k_p , k_e , and k_μ denote the Fermi momenta of neutrons, protons, electrons, and muons, respectively. Notice that the quantum many-body effects are already included in these chemical potentials. The rest lepton masses are $m_e = 0.511$ MeV and $m_\mu = 105.7$ MeV. The lepton densities are related to the corresponding Fermi momenta via the relations $\rho_{e,\mu} = k_{e,\mu}^3/(3\pi^2)$. Also, the neutron-star core should preserve the baryon number conservation and ensure the electric neutrality given by two equalities:

$$\rho_B^* = \rho_n + \rho_p, \quad (58)$$

$$Q_p + Q_e + Q_\mu = \rho_p - \rho_e - \rho_\mu = 0. \quad (59)$$

Here, Q_p , Q_e , and Q_μ are the electric charges carried by proton, electron, and muon, respectively. Making use of Eqs. (52-59), we determine the densities of neutrons, protons, electrons, and muons at a given total density ρ_B^* , which then generates a more realistic EOS for neutron stars that satisfies the β equilibrium:

$$\epsilon_\beta = \epsilon + \sum_{l=e,\mu} \frac{1}{\pi^2} \int_0^{k_l} k^2 dk \sqrt{k_l^2 + m_l^2}, \quad (60)$$

$$P_\beta = P + \sum_{l=e,\mu} \frac{1}{3\pi^2} \int_0^{k_l} dk \frac{k^4}{\sqrt{k_l^2 + m_l^2}}. \quad (61)$$

IV. MASS-RADIUS RELATION, TIDAL DEFORMABILITY, AND SOUND SPEED

The relation between the mass M and radius R of neutron stars can be obtained by inserting the EOS into the Tolman-Oppenheimer-Volkoff (TOV) equations [47, 48] given by

$$\frac{dP(r)}{dr} = -\frac{[P(r) + \epsilon(r)][M(r) + 4\pi r^3 P(r)]}{r[r - 2M(r)]}, \quad (62)$$

$$\frac{dM(r)}{dr} = 4\pi r^2 \epsilon(r). \quad (63)$$

Here, $M(r)$ represents the gravitational mass enclosed within a sphere of radius r and $\epsilon(r)$ and $P(r)$ are the energy density and the pressure at r , respectively.

In addition to the M - R relation, tidal deformability is another important observable quantity that is frequently used to probe the interior structure of neutron stars. This quantity measures the deformation of a neutron star under the influence of an external gravitational field exerted by other stars. The tidal deformability can be quantified by a dimensionless parameter [49, 50]:

$$\Lambda = \frac{2}{3} k_2 C^{-5}, \quad (64)$$

where $C = M/R$ is the compactness parameter and k_2 , related to the neutron star EOS, refers to the second-order Love number. Detailed calculations and derivations of k_2 can be found in Refs. [49, 50].

After carrying out extensive calculations, we find a few suitable sets of parameters and show them in Table I. Among these models, the $\sigma\omega\rho 2$ model appears to be an ideal candidate. The values of ρ_{B0} , E_b , m_N^* , K , and E_s produced by this model are very consistent with experiments. But the slope $L_s = 87.56$ MeV seems too large. Accordingly, the tidal deformability $\Lambda_{1.4}$ for a neutron star with mass $1.4 M_\odot$ is also unrealistically large.

To get more realistic L_s and $\Lambda_{1.4}$, we replace constant g_ρ by a density dependent function [18, 51] given by

$$\Gamma_\rho = g_\rho \exp \left[-a_\rho \left(\frac{\rho_B^*}{\rho_{B0}} - 1 \right) \right], \quad (65)$$

where a_ρ is the sixth tuning parameter for the $\sigma\omega\rho 2$ model. As a_ρ grows from zero, the values of ρ_{B0} , E_b , m_N^* , K , and E_s listed in Table I remain unchanged, but L_s and $\Lambda_{1.4}$ are both substantially reduced, as shown by Table II. In Fig. 4, we present the M - R curves determined by $\sigma\omega\rho 2$ model with different values of L_s . Smaller values of L_s and $\Lambda_{1.4}$ correspond to smaller radii.

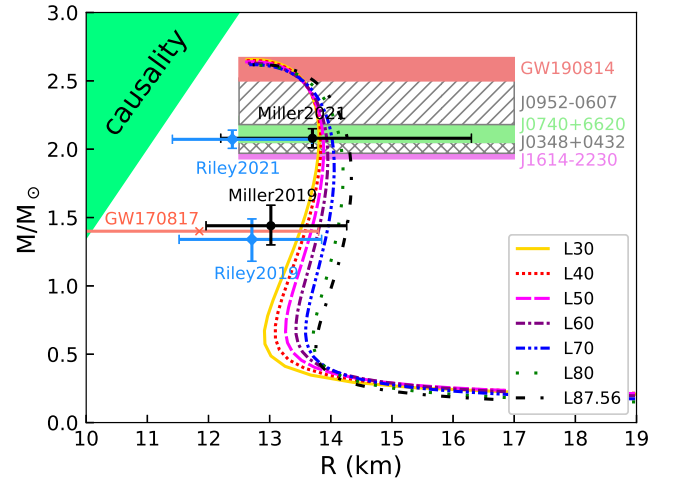


FIG. 4: Comparison between the theoretical results of the M - R relations obtained from $\sigma\omega\rho 2$ model and astrophysical observations of neutron stars.

Shown in Fig. 4 are some recently observed values

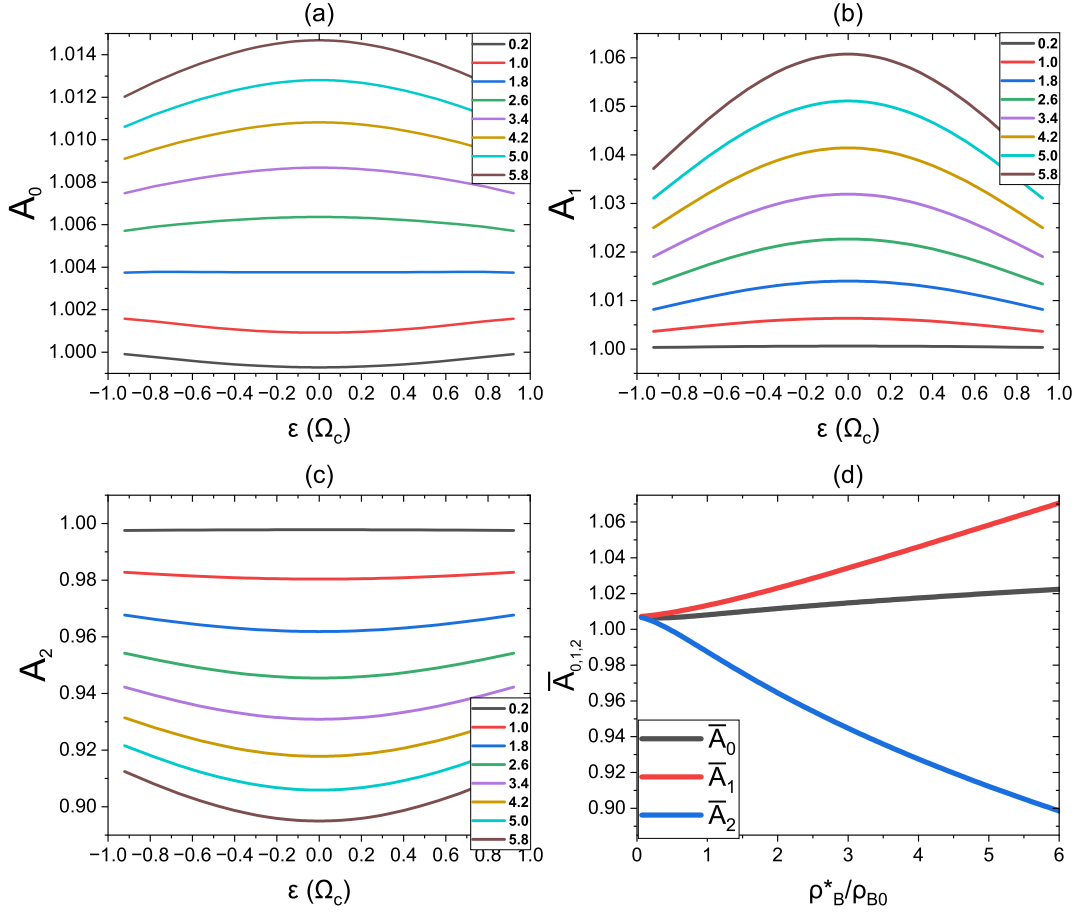
of neutron star masses and radii. One can see that

TABLE I: Simulated model parameters and nuclear quantities computed at saturation density.

Model	g_σ	g_ω	g_ρ	g_δ	m_σ^*/m_σ	Λ_c
$\sigma\omega$	11.2852	11.4243	0.0	0.0	1.2204	2.4672
$\sigma\omega\rho 1$	16.8355	10.9381	8.0028	0.0	1.9501	2.0
$\sigma\omega\rho 2$	17.5758	11.3153	6.5393	0.0	1.9355	1.6011
$\sigma\omega\rho\delta$	17.5758	11.3153	6.5393	1.3554	1.9355	1.6011
	ρ_{B0} (fm $^{-3}$)	E_b (MeV)	m_N^* (m_N)	K (MeV)	E_s (MeV)	L_s (MeV)
$\sigma\omega$	0.1580	-16.4176	0.6327	250.1615	19.0599	57.8220
$\sigma\omega\rho 1$	0.1599	-16.8985	0.6699	260.6649	34.3386	101.4963
$\sigma\omega\rho 2$	0.1597	-16.4255	0.6462	220.5497	28.9727	87.5612
$\sigma\omega\rho\delta$	0.1597	-16.8108	0.6457	221.3642	28.0002	85.4057

TABLE II: Dependence of L_s (at saturation density) and $\Lambda_{1.4}$ on the tuning parameter a_ρ for the $\sigma\omega\rho 2$ model.

Model	$L_{87.56}$	L_{80}	L_{70}	L_{60}	L_{50}	L_{40}	L_{30}
a_ρ	0	0.1123	0.2610	0.4097	0.5583	0.7070	0.8557
L_s (MeV)	87.56	80	70	60	50	40	30
$\Lambda_{1.4}$	1225	1112	1038	954	903	872	847

FIG. 5: Behavior of renormalization functions for $\sigma\omega\rho 2$ model at $L_s = 40$ MeV and $a_\rho = 0.7070$. (a - c) Energy dependence of $A_0(\epsilon)$, $A_1(\epsilon)$, and $A_2(\epsilon)$ for eight densities: $0.2\rho_{B0}$, $1.0\rho_{B0}$, $1.8\rho_{B0}$, $2.6\rho_{B0}$, $3.4\rho_{B0}$, $4.2\rho_{B0}$, $5.0\rho_{B0}$, $5.8\rho_{B0}$. (d) Density dependence of averaged quantities \bar{A}_0 , \bar{A}_1 , and \bar{A}_2 .

the three M - R curves obtained with $L_s = 30$ MeV, $L_s = 40$ MeV, and $L_s = 50$ MeV are very consistent with the masses and radii extracted from the GW170817 event generated by the binary neutron star merger ($R_{1.4M_\odot} = 11.85^{+1.95}_{-1.95}$ km) [52], those from PSR J0030+0451 ($M = 1.44^{+0.15}_{-0.14} M_\odot$ and $R = 13.02^{+1.24}_{-1.06}$ km reported by Miller *et al.* [31] and $M = 1.34^{+0.15}_{-0.16} M_\odot$ and $R = 12.71^{+1.14}_{-1.19}$ km reported by Riley *et al.* [32]), and those from PSR J0740+6620 ($M = 2.08^{+0.07}_{-0.07} M_\odot$ and $R = 13.7^{+2.6}_{-1.5}$ km reported by Miller *et al.* [33] and $M = 2.072^{+0.067}_{-0.066} M_\odot$ and $R = 12.39^{+1.30}_{-0.98}$ km reported by Riley *et al.* [34]). These three M - R curves also satisfy the mass constraints of PSR J1614-2230 ($1.97^{+0.04}_{-0.04} M_\odot$) [35], PSR J0348+0432 ($2.01^{+0.04}_{-0.04} M_\odot$) [36], PSR J0740+6620 ($2.14^{+0.10}_{-0.09} M_\odot$) [37], and PSR J0952-0607 ($2.35^{+0.17}_{-0.17} M_\odot$) [38].

Recently, two binary compact objects were detected from the gravitational wave event GW190814 [53]. The heavier object has a mass $\approx 23 M_\odot$ and was soon recognized as a black hole [53]. The other one has a much smaller mass about $(2.50 - 2.67)M_\odot$. It remains an open puzzle whether the lighter one is the heaviest known neutron star or the lightest black hole ever found. The maximal mass predicted by the $L30$, $L40$, $L50$ curves plotted in Fig. 4 is $M_{\max} \approx 2.67M_\odot$. Thus, our theoretical results point to the former possibility and indicate that such a putative massive neutron star would have a radius within the range of $(12.65 - 13.55)$ km. A more definite conclusion might be drawn by measuring its radius with high precision.

For $L_s = 40$ MeV, our theoretical result $\Lambda_{1.4} = 872$ satisfies the constraint $458 \leq \Lambda_{1.4} \leq 889$ inferred from GW190814 if the low-mass compact object is assumed to be a neutron star [53]. In this view, the magnitudes of M_{\max} and $\Lambda_{1.4}$ obtained in our calculations are consistent with each other. However, the result $\Lambda_{1.4} = 872$ is out of the range $70 \leq \Lambda_{1.4} \leq 580$ extracted from GW170817 [29, 30]. At present, the precise value of $\Lambda_{1.4}$ remains largely uncertain due to the insufficiency of observational data on the tidal deformability. Analysis based on diverse assumptions and approximations often yield conflicting results of $\Lambda_{1.4}$. More comprehensive gravitational wave events from binary mergers are required to impose more stringent constraints on $\Lambda_{1.4}$.

We plot the numerical solutions of $A_{0,1,2}(\epsilon)$ in Fig. 5 for symmetric nuclear matter at $L_s = 40$ MeV and $a_\rho = 0.7070$. Their properties in neutron-dominated neutron star matter are similar. One can see from Fig. 5(d) that \bar{A}_0 , \bar{A}_1 , and \bar{A}_2 are close but never equal to unity at very low densities. With the increase of the density, \bar{A}_0 , \bar{A}_1 , and \bar{A}_2 deviate considerably from unity. Quantum many-body effects are more significant at higher densities. However, they are present at all densities. We find that $A_{0,1,2}(\epsilon)$ have convergent solutions within the density range $\rho_B^* < 6\rho_{B0}$, which is much wider than the density range covered by χ EFT.

The speed of sound c_s is also a pivotal factor in the de-

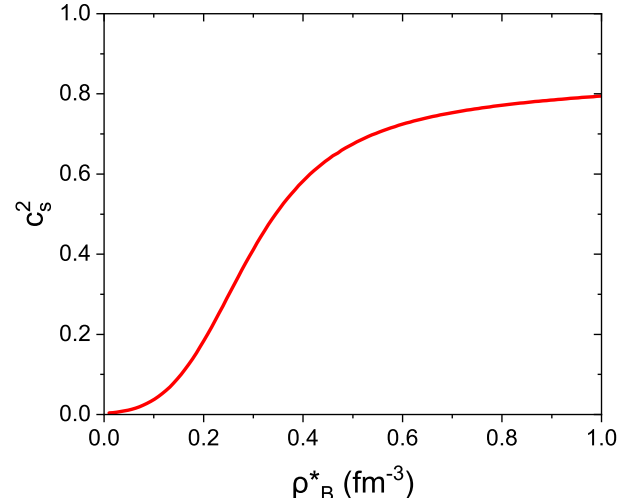


FIG. 6: The speed of sound squared as a function of neutron density in a pure neutron matter. Here, we have made the speed of light squared $c^2 = 1$.

scription of neutron stars as it characterizes the stiffness and incompressibility of the EOS [1]. Causality requires that c_s must be smaller than the speed of light c . We have computed the sound speed squared, defined by

$$c_s^2 = \frac{\partial P(\epsilon)}{\partial \epsilon}, \quad (66)$$

for a pure neutron matter. The density dependence of c_s^2 is depicted in Fig. 6. Evidently, the ratio c_s^2/c^2 is always smaller than unity. As the neutron density increases, the ratio converges towards a consistent value of 0.8. This conclusion also holds for symmetric nuclear matter and neutron star matter. Therefore, the causality is ensured in all of our results.

V. SUMMARY AND DISCUSSION

In summary, we propose a nonperturbative approach to incorporate the effects of quantum many-body correlations into the EOS of neutron stars. The key step of this approach is to solve the self-consistent DS equation of the renormalized neutron propagator $G(k)$, which takes into account the many-body correlation effects through three renormalization functions. After carrying out extensive calculations, we select out a relatively simple σ - ω - ρ model to describe the physics of dense neutron star matter. We show that the EOS generated from this model leads to several observable quantities of saturation nuclear matter that are consistent with experiments. The M - R relation determined by such an EOS is comparable with some recent astrophysical observations.

Our approach can be extended and further improved in several directions. First, the zero-temperature EOS

obtained in this paper can be generalized to finite temperatures. Finite temperature EOS may have applications in the description of protoneutron stars [54] and binary neutron star mergers [55]. Second, our approach can be employed to examine the influence of additional exotic degrees of freedom, such as hyperons [1, 13] and Δ -isobars [56, 57], that might be present in the high-density region of neutron star core. These additional degrees of freedom may soften the EOS and decrease the radii and/or the maximum mass M_{max} of neutron stars. Third, the momentum dependence of the current vertex functions Υ_I , $\Gamma_{\gamma\nu}$, $\Theta_{\tau_3\gamma\nu}$, and Ω_{τ_3} (see the last three paragraphs of the Appendix A for a detailed explanation) need to be taken into account. One possible way to do this is to expand these current vertex functions around the Fermi momentum k_F by taking $|\mathbf{k}| - k_F$ as a small parameter. Finally, the EOS obtained in this paper is calculated based on a combination of the nonperturbative DS equation and RMFT. In an effort to go beyond such a hybrid route, we would directly utilize the renormalized neutron propagator $G(k)$, extracted from the solutions of its DS equation, to compute thermodynamic quantities and EOS by virtue of the LW functional [45].

As mentioned in Sec. IV, the tidal deformability $\Lambda_{1.4}$ generated by our EOS appears to be considerably larger than the result constrained by recent gravitational wave events. In the future, we will examine whether a more realistic value of $\Lambda_{1.4}$ could be obtained after some of the improvements discussed above are accomplished.

The analysis in Sec. III A and IV indicates that our approach offers a formalism different from RMFT. It turns out that our results do not reduce to RMFT results at any density. Given the impressive success of RMFT in the description of finite nuclei, one might wonder whether our approach can be used to study finite nuclei. Our nonperturbative formalism is rooted in the quantum many-body theory, which is supposed to be applicable to an equilibrium or near-equilibrium system that has a large number ($\approx 10^{23}$) of particles. The neutron-star matter can be approximately considered as such a system. The lower limit $|\mathbf{q}| = 0$ for meson momentum \mathbf{q} implies that the neutron-star matter is assumed to have a very large volume. However, finite nuclei means a small system containing typically dozens of nucleons. The nonperturbative formalism cannot be directly employed to deal with finite nuclei. In order to embody the smallness of finite nuclei volume, the meson momentum $|\mathbf{q}|$ should be larger than some critical value Λ_{IR} , which serves as an infrared cutoff. Accordingly, the integration range $|\mathbf{q}| \in [0, \Lambda_c k_F]$ should be replaced by $|\mathbf{q}| \in [\Lambda_{\text{IR}}, \Lambda_c k_F]$. Then one could solve the integral equations of $A_{0,1,2}(\varepsilon)$ and utilize the solutions to describe the properties of finite nuclei. Our present work concentrates on the many-body correlation effects in neutron-star matter. It would be of interest to examine whether the properties of finite nuclei can be described by a reformed version of our formalism.

We finally remark on the application of our approach to the investigation of neutron superfluidity. It is univer-

sally believed [58, 59] that neutron superfluid exists in neutron stars and is responsible for the observed glitch phenomena. Superfluid also plays a significant role in the thermal evolution of neutron stars [59]. Unfortunately, both the superfluid gap Δ_n and transition temperature T_c have not been unambiguously determined to date. Previous calculations of Δ_n and T_c are predominantly based on BCS mean-field theory [58, 59]. The pairing potential $V(\mathbf{r})$ used in such calculations is obtained from the experimental data of two-body scattering phase shift [58, 59]. These mean-field calculations are problematic for several reasons. The first one is that the instantaneous pairing potential entirely neglects the retardation of meson propagation. The second one is the absence of the in-medium effect. Moreover, BCS mean-field theory fails to include the influence of neutron damping and neutron velocity/mass renormalization. Another obvious shortcoming of BCS-level calculations is that the pairing potential $V(\mathbf{r})$ is entirely unknown at high densities due to the absence of experimental data of scattering phase shift above 350 MeV. For a massive neutron star, the relevant neutron energy in the high-density region could be much greater than 350 MeV. For these reasons, it is important to study neutron superfluidity beyond BCS mean-field theory. The nonperturbative approach that we develop in this paper is capable of including the effects ignored in previous BCS-level calculations, such as the neutron damping, the neutron velocity/mass renormalization, the retardation of meson propagation, as well as the in-medium screening (it can be embodied by adding the polarization functions to the meson propagators). Furthermore, our DS equation has as convergent solutions even when the neutron density is as high as $6\rho_B$, which is far beyond 350 MeV. We thus expect that our approach provides a more efficient framework for the theoretical study of neutron superfluidity than the BCS mean-field theory. This issue will be addressed in a separate work.

Some alternative forms of exotic matter, such as quark stars and hybrid stars, have been proposed to understand the physics of neutron stars [1]. Especially, quark degrees of freedom may exist in the cores of certain neutron stars [60, 61]. The interactions of quarks with mesons or gluons might result in significant quantum many-body effects. It would be interesting to study such effects by employing an extended version of the nonperturbative DS equation framework.

VI. ACKNOWLEDGEMENT

We thank Sophia Han, Wei-Zhou Jiang, and Ang Li for helpful discussions. This work is supported by the National Natural Science Foundation of China under Grant No. 12073026, the Anhui Natural Science Foundation under Grant No. 2208085MA11, and the Fundamental Research Funds for the Central Universities.

Appendix A: Derivation of Dyson-Schwinger equation of nucleon propagator

Here we provide a detailed derivation of the DS equation of the neutron propagator given by Eq. (4). The derivation will be performed within the path-integral framework of quantum field theory. The Lagrangian density Eq. (1) can be re-written as

$$\begin{aligned}
\mathcal{L}_T = & \bar{\psi}(i\partial_\mu\gamma^\mu - m_N)\psi + \frac{1}{2}\partial_\mu\sigma\partial^\mu\sigma - \frac{1}{2}m_\sigma^2\sigma^2 \\
& - \frac{1}{4}\omega_{\mu\nu}\omega^{\mu\nu} + \frac{1}{2}m_\omega^2\omega_\mu\omega^\mu \\
& - \frac{1}{4}\rho_{3\mu\nu}\rho_3^{\mu\nu} + \frac{1}{2}m_\rho^2\rho_{3\mu}\rho_3^\mu \\
& + \frac{1}{2}\partial_\mu\delta_3\partial^\mu\delta_3 - \frac{1}{2}m_\delta^2\delta_3^2 \\
& + g_\sigma\sigma\bar{\psi}\psi - g_\omega\omega_\mu\bar{\psi}\gamma^\mu\psi \\
& - \frac{1}{2}g_\rho\rho_{3\mu}\bar{\psi}\tau_3\gamma^\mu\psi + g_\delta\delta_3\bar{\psi}\tau_3\psi \\
& + \bar{\eta}\psi + \bar{\psi}\eta + J_\sigma\sigma + J_\omega^\mu\omega_\mu \\
& + J_\rho^\mu\rho_{3\mu} + J_\delta\delta_3.
\end{aligned} \tag{A1}$$

Here, we have introduced several external sources J_σ , J_ω^μ , J_ρ^μ , J_δ , $\bar{\eta}$, and η , which are associated with fields σ , ω_μ , $\rho_{3\mu}$, δ_3 , ψ , and $\bar{\psi}$, respectively.

To help readers understand the calculational details, we list some basic rules of functional integral [39, 41]. All the correlation functions are generated from three quantities: the partition function $Z[J_\sigma, J_\omega^\mu, J_\rho^\mu, J_\delta, \bar{\eta}, \eta]$, the generating functional $W[J_\sigma, J_\omega^\mu, J_\rho^\mu, J_\delta, \bar{\eta}, \eta]$ and the generating functional $\Xi[\sigma, \omega_\mu, \rho_{3\mu}, \delta_3, \psi, \bar{\psi}]$. They are defined as:

$$\begin{aligned}
Z[J_\sigma, J_\omega^\mu, J_\rho^\mu, J_\delta, \bar{\eta}, \eta] &= \int \mathcal{D}\sigma \mathcal{D}\omega_\mu \mathcal{D}\rho_{3\mu} \mathcal{D}\delta_3 \mathcal{D}\bar{\psi} \mathcal{D}\psi \\
&\quad \times \exp\left(i \int d^4z \mathcal{L}_T\right), \\
W[J_\sigma, J_\omega^\mu, J_\rho^\mu, J_\delta, \bar{\eta}, \eta] &= -i \ln Z[J_\sigma, J_\omega^\mu, J_\rho^\mu, J_\delta, \bar{\eta}, \eta], \\
\Xi[\sigma, \omega_\mu, \rho_{3\mu}, \delta_3, \psi, \bar{\psi}] &= W[J_\sigma, J_\omega^\mu, J_\rho^\mu, J_\delta, \bar{\eta}, \eta] \\
&\quad - \int (J_\sigma\sigma + J_\omega^\mu\omega_\mu \\
&\quad + J_\rho^\mu\rho_{3\mu} + J_\delta\delta_3 + \bar{\eta}\psi + \bar{\psi}\eta).
\end{aligned}$$

Here, $z = (t, \mathbf{z})$ is (1 + 3)-dimensional position vector. The following identities will be frequently used:

$$\begin{aligned}
\frac{\delta W}{\delta J_\sigma} &= \langle \sigma \rangle, & \frac{\delta W}{\delta J_\omega^\mu} &= \langle \omega_\mu \rangle, & \frac{\delta W}{\delta J_\rho^\mu} &= \langle \rho_{3\mu} \rangle, \\
\frac{\delta W}{\delta J_\delta} &= \langle \delta_3 \rangle, & \frac{\delta W}{\delta \bar{\eta}} &= -\langle \bar{\psi} \rangle, & \frac{\delta W}{\delta \eta} &= \langle \psi \rangle, \\
\frac{\delta \Xi}{\delta \sigma} &= -J_\sigma, & \frac{\delta \Xi}{\delta \omega_\mu} &= -J_\omega^\mu, & \frac{\delta \Xi}{\delta \rho_{3\mu}} &= -J_\rho^\mu, \\
\frac{\delta \Xi}{\delta \delta_3} &= -J_\delta, & \frac{\delta \Xi}{\delta \bar{\psi}} &= \bar{\eta}, & \frac{\delta \Xi}{\delta \psi} &= -\eta.
\end{aligned}$$

Generating functional W generates various connected correlation functions, whereas Ξ generates all the irreducible proper vertices. In Lagrangian density \mathcal{L}_T there are four different interactions between mesons and nucleons, denoted by σN , ωN , $\rho_0 N$, and $\delta_0 N$, respectively. We presume the system exhibits translational invariance. The full (exact) nucleon propagator $G(z - z_1)$, the full σ -meson propagator $D(z - z_2)$, the full ω -meson propagator $F^{\mu\nu}(z - z_2)$, the full ρ_0 -meson propagator $V^{\mu\nu}(z - z_2)$, and the full δ_0 -meson propagator $C(z - z_2)$ are defined in terms of W in order by

$$\begin{aligned}
G(z - z_1) &\equiv -i\langle \psi(z)\bar{\psi}(z_1) \rangle = \frac{\delta^2 W}{\delta \bar{\eta}(z)\delta \eta(z_1)}, \\
D(z - z_2) &\equiv -i\langle \sigma(z)\sigma^\dagger(z_2) \rangle = -\frac{\delta^2 W}{\delta J_\sigma(z)\delta J_\sigma(z_2)}, \\
F^{\mu\nu}(z - z_2) &\equiv -i\langle \omega^\mu(z)\omega^{\nu\dagger}(z_2) \rangle = -\frac{\delta^2 W}{\delta J_\omega^\mu(z)\delta J_\omega^\nu(z_2)}, \\
V^{\mu\nu}(z - z_2) &\equiv -i\langle \rho_3^\mu(z)\rho_3^{\nu\dagger}(z_2) \rangle = -\frac{\delta^2 W}{\delta J_\rho^\mu(z)\delta J_\rho^\nu(z_2)}, \\
C(z - z_2) &\equiv -i\langle \delta_3^\mu(z)\delta_3^{\dagger}(z_2) \rangle = -\frac{\delta^2 W}{\delta J_\delta(z)\delta J_\delta(z_2)}.
\end{aligned}$$

The vertex corrections to nucleon-meson interactions can be described by four three-point correlation functions $\langle \sigma\psi\bar{\psi} \rangle$, $\langle \omega^\mu\psi\bar{\psi} \rangle$, $\langle \rho_3^\mu\psi\bar{\psi} \rangle$, and $\langle \delta_3\psi\bar{\psi} \rangle$, which are defined via W and Ξ as follows:

$$\langle \sigma\psi\bar{\psi} \rangle \equiv \frac{\delta^3 W}{\delta J_\sigma\delta \bar{\eta}\delta \eta} = -DG \frac{\delta^3 \Xi}{\delta \sigma\delta \bar{\psi}\delta \psi} G, \tag{A2}$$

$$\langle \omega^\mu\psi\bar{\psi} \rangle \equiv \frac{\delta^3 W}{\delta J_\omega^\mu\delta \bar{\eta}\delta \eta} = -F_{\mu\nu}G \frac{\delta^3 \Xi}{\delta \omega_\nu\delta \bar{\psi}\delta \psi} G, \tag{A3}$$

$$\langle \rho_3^\mu\psi\bar{\psi} \rangle \equiv \frac{\delta^3 W}{\delta J_\rho^\mu\delta \bar{\eta}\delta \eta} = -V_{\mu\nu}G \frac{\delta^3 \Xi}{\delta \rho_{3\nu}\delta \bar{\psi}\delta \psi} G, \tag{A4}$$

$$\langle \delta_3\psi\bar{\psi} \rangle \equiv \frac{\delta^3 W}{\delta J_\delta\delta \bar{\eta}\delta \eta} = -CG \frac{\delta^3 \Xi}{\delta \delta_3\delta \bar{\psi}\delta \psi} G. \tag{A5}$$

Next, we derive the DS equation of the full nucleon propagator with the help of the above identities. Given that Z is invariant under an arbitrary infinitesimal variation of spinor field $\bar{\psi}$, i.e.,

$$\int \mathcal{D}\sigma \mathcal{D}\omega_\mu \mathcal{D}\rho_{3\mu} \mathcal{D}\delta_3 \mathcal{D}\bar{\psi} \mathcal{D}\psi \frac{\delta}{\delta \bar{\psi}} \exp\left(i \int d^4z \mathcal{L}_T\right) = 0,$$

we find that the following relation holds:

$$\begin{aligned}
&\langle (i\partial_\mu\gamma^\mu - m_N)\psi(z) \rangle + \langle \eta(z) \rangle \\
&+ \langle g_\sigma\sigma(z)\psi(z) \rangle - \langle g_\omega\omega_\mu(z)\gamma^\mu\psi(z) \rangle \\
&- \langle \frac{g_\rho}{2}\rho_{3\mu}(z)\tau_3\gamma^\mu\psi(z) \rangle + \langle g_\delta\delta_3(z)\tau_3\psi(z) \rangle = 0.
\end{aligned}$$

This relation is equivalent to

$$\begin{aligned}
-\eta(z) = & (i\partial_\mu\gamma^\mu - m_N)\frac{\delta W}{\delta\bar{\eta}(z)} - ig_\sigma\frac{\delta^2 W}{\delta J_\sigma(z)\delta\bar{\eta}(z)} + g_\sigma\frac{\delta W}{\delta J_\sigma(z)}\frac{\delta W}{\delta\bar{\eta}(z)} + ig_\omega\gamma^\mu\frac{\delta^2 W}{\delta J_\omega^\mu(z)\delta\bar{\eta}(z)} - g_\omega\frac{\delta W}{\delta J_\omega^\mu(z)}\gamma^\mu\frac{\delta W}{\delta\bar{\eta}(z)} \\
& + i\frac{g_\rho}{2}\tau_3\gamma^\mu\frac{\delta^2 W}{\delta J_\rho^\mu(z)\delta\bar{\eta}(z)} - \frac{g_\rho}{2}\frac{\delta W}{\delta J_\rho^\mu(z)}\tau_3\gamma^\mu\frac{\delta W}{\delta\bar{\eta}(z)} - ig_\delta\tau_3\frac{\delta^2 W}{\delta J_\delta(z)\delta\bar{\eta}(z)} + g_\delta\frac{\delta W}{\delta J_\delta(z)}\tau_3\frac{\delta W}{\delta\bar{\eta}(z)}. \quad (A6)
\end{aligned}$$

Two terms of the above equation vanish upon removing sources and can be directly omitted. Carrying out functional derivatives of both sides of this equation with respect to $\eta(z_2)$ and using the identities (A2-A5) leads to

$$\begin{aligned}
\delta(z - z_2) = & (i\partial_\mu\gamma^\mu - m_N)\frac{\delta^2 W}{\delta\bar{\eta}(z)\delta\eta(z_2)} - ig_\sigma\frac{\delta^3 W}{\delta J_\sigma(z)\delta\bar{\eta}(z)\delta\eta(z_2)} + ig_\omega\gamma^\mu\frac{\delta^3 W}{\delta J_\omega^\mu(z)\delta\bar{\eta}(z)\delta\eta(z_2)} \\
& + i\frac{g_\rho}{2}\tau_3\gamma^\mu\frac{\delta^3 W}{\delta J_\rho^\mu(z)\delta\bar{\eta}(z)\delta\eta(z_2)} - ig_\delta\tau_3\frac{\delta^3 W}{\delta J_\delta(z)\delta\bar{\eta}(z)\delta\eta(z_2)} \\
= & (i\partial_\mu\gamma^\mu - m_N)G(z - z_2) + ig_\sigma\int dz_1dz_3dz_4D(z - z_3)G(z - z_1)\frac{\delta^3\Xi}{\delta\sigma(z_3)\delta\bar{\psi}(z_1)\delta\psi(z_4)}G(z_4 - z_2) \\
& - ig_\omega\int dz_1dz_3dz_4\gamma_\mu F^{\mu\nu}(z - z_3)G(z - z_1)\frac{\delta^3\Xi}{\delta\omega^\nu(z_3)\delta\bar{\psi}(z_1)\delta\psi(z_4)}G(z_4 - z_2) \\
& - i\frac{g_\rho}{2}\int dz_1dz_3dz_4\tau_3\gamma_\mu V^{\mu\nu}(z - z_3)G(z - z_1)\frac{\delta^3\Xi}{\delta\rho_3^\nu(z_3)\delta\bar{\psi}(z_1)\delta\psi(z_4)}G(z_4 - z_2) \\
& + ig_\delta\int dz_1dz_3dz_4\tau_3C(z - z_3)G(z - z_1)\frac{\delta^3\Xi}{\delta\delta_3(z_3)\delta\bar{\psi}(z_1)\delta\psi(z_4)}G(z_4 - z_2).
\end{aligned}$$

This equation can be further expressed as

$$\begin{aligned}
& G^{-1}(z - z_2) \\
= & (i\partial_\mu\gamma^\mu - m_N)\delta(z - z_2) \\
& + ig_\sigma\int dz_1dz_3D(z - z_3)G(z - z_1)\Upsilon(z_3, z_1, z_2) \\
& - ig_\omega\int dz_1dz_3\gamma_\mu F^{\mu\nu}(z - z_3)G(z - z_1)\Gamma_\nu(z_3, z_1, z_2) \\
& - i\frac{g_\rho}{2}\int dz_1dz_3\tau_3\gamma_\mu V^{\mu\nu}(z - z_3)G(z - z_1)\Theta_\nu(z_3, z_1, z_2) \\
& + ig_\delta\int dz_1dz_3\tau_3C(z - z_3)G(z - z_1)\Omega(z_3, z_1, z_2). \quad (A7)
\end{aligned}$$

Here, we have defined a truncated (all external legs being dropped) σN interaction vertex function

$$\Upsilon(z_3, z_1, z_2) = \frac{\delta^3\Xi}{\delta\sigma(z_3)\delta\bar{\psi}(z_1)\delta\psi(z_2)}, \quad (A8)$$

a truncated ωN interaction vertex function

$$\Gamma_\nu(z_3, z_1, z_2) = \frac{\delta^3\Xi}{\delta\omega^\nu(z_3)\delta\bar{\psi}(z_1)\delta\psi(z_2)}, \quad (A9)$$

a truncated $\rho_0 N$ interaction vertex function

$$\Theta_\nu(z_3, z_1, z_2) = \frac{\delta^3\Xi}{\delta\rho_3^\nu(z_3)\delta\bar{\psi}(z_1)\delta\psi(z_2)}, \quad (A10)$$

and a truncated $\delta_0 N$ interaction vertex function

$$\Omega(z_3, z_1, z_2) = \frac{\delta^3\Xi}{\delta\delta_3(z_3)\delta\bar{\psi}(z_1)\delta\psi(z_2)}. \quad (A11)$$

The propagators are Fourier transformed as

$$\begin{aligned}
G(z - z_1) &= \int \frac{d^4k}{(2\pi)^4} e^{-ik(z-z_1)} G(k), \\
D(z - z_2) &= \int \frac{d^4q}{(2\pi)^4} e^{-iq(z-z_2)} D(q), \\
F^{\mu\nu}(z - z_2) &= \int \frac{d^4q}{(2\pi)^4} e^{-iq(z-z_2)} F^{\mu\nu}(q), \\
V^{\mu\nu}(z - z_2) &= \int \frac{d^4q}{(2\pi)^4} e^{-iq(z-z_2)} V^{\mu\nu}(q), \\
C(z - z_2) &= \int \frac{d^4q}{(2\pi)^4} e^{-iq(z-z_2)} C(q).
\end{aligned}$$

If the translational invariance is preserved, interaction vertex functions are Fourier transformed as

$$\begin{aligned}
& \Upsilon(z_1, z, z_2) \equiv \Upsilon(z_1 - z, z - z_2) \\
= & \int \frac{d^4qd^4k}{(2\pi)^8} e^{-i(k+q)(z_1-z)} e^{-ik(z-z_2)} \Upsilon(q, k), \\
& \Gamma_\nu(z_1, z, z_2) \equiv \Gamma_\nu(z_1 - z, z - z_2) \\
= & \int \frac{d^4qd^4k}{(2\pi)^8} e^{-i(k+q)(z_1-z)} e^{-ik(z-z_2)} \Gamma_\nu(q, k), \\
& \Theta_\nu(z_1, z, z_2) \equiv \Theta_\nu(z_1 - z, z - z_2) \\
= & \int \frac{d^4qd^4k}{(2\pi)^8} e^{-i(k+q)(z_1-z)} e^{-ik(z-z_2)} \Theta_\nu(q, k), \\
& \Omega(z_1, z, z_2) \equiv \Omega(z_1 - z, z - z_2) \\
= & \int \frac{d^4qd^4k}{(2\pi)^8} e^{-i(k+q)(z_1-z)} e^{-ik(z-z_2)} \Omega(q, k).
\end{aligned}$$

Performing Fourier transformation of Eq. (A7) leads us to the DS equation obeyed by the nucleon propagator:

$$\begin{aligned}
G^{-1}(k) = & G_0^{-1}(k) + ig_\sigma \int \frac{d^4q}{(2\pi)^4} G(k+q) D(q) \Upsilon(q, k) \\
& - ig_\omega \int \frac{d^4q}{(2\pi)^4} \gamma_\mu G(k+q) F^{\mu\nu}(q) \Gamma_\nu(q, k) \\
& - i\frac{g_\rho}{2} \int \frac{d^4q}{(2\pi)^4} \tau_3 \gamma_\mu G(k+q) V^{\mu\nu}(q) \Theta_\nu(q, k) \\
& + ig_\delta \int \frac{d^4q}{(2\pi)^4} \tau_3 G(k+q) C(q) \Omega(q, k). \quad (\text{A12})
\end{aligned}$$

Here, the free nucleon propagator has the form

$$G_0(k) = \frac{1}{k_\mu \gamma^\mu - m_N}. \quad (\text{A13})$$

The free propagators of σ , ω , ρ_0 , and δ_0 are

$$D_0(q) = \frac{1}{q^2 - m_\sigma^2}, \quad (\text{A14})$$

$$F_0^{\mu\nu}(q) = \frac{-1}{q^2 - m_\omega^2} \left(g^{\mu\nu} - \frac{q^\mu q^\nu}{m_\omega^2} \right), \quad (\text{A15})$$

$$V_0^{\mu\nu}(q) = \frac{-1}{q^2 - m_\rho^2} \left(g^{\mu\nu} - \frac{q^\mu q^\nu}{m_\rho^2} \right), \quad (\text{A16})$$

$$C_0(q) = \frac{1}{q^2 - m_\delta^2}. \quad (\text{A17})$$

The DS equations of meson propagators can be derived in an analogous way [39, 41]. We will not give the derivational details and just present their final expressions:

$$\begin{aligned}
D^{-1}(q) = & D_0^{-1}(q) - ig_\sigma \int \frac{d^4k}{(2\pi)^4} \text{Tr}[G(k+q) \Upsilon(q, k) G(k)], \\
F_{\mu\nu}^{-1}(q) = & F_{0\mu\nu}^{-1}(q) + ig_\omega \int \frac{d^4k}{(2\pi)^4} \text{Tr}[\gamma^\mu G(k+q) \Gamma^\nu(q, k) G(k)], \\
V_{\mu\nu}^{-1}(q) = & V_{0\mu\nu}^{-1}(q) + i\frac{g_\rho}{2} \int \frac{d^4k}{(2\pi)^4} \text{Tr}[\tau_3 \gamma^\mu G(k+q) \Theta^\nu(q, k) G(k)], \\
C^{-1}(q) = & C_0^{-1}(q) - ig_\delta \int \frac{d^4k}{(2\pi)^4} \text{Tr}[\tau_3 G(k+q) \Omega(q, k) G(k)].
\end{aligned}$$

The vertex functions $\Upsilon(q, k)$, $\Gamma_\nu(q, k)$, $\Theta_\nu(q, k)$, and $\Omega(q, k)$ satisfy their own DS equations, which are related to an infinite number of multipoint correlation functions through an infinite number of DS equations. The complete set of DS equations are exact, but are apparently too complicated to handle.

The mutually coupled DS equations can be simplified by using a method proposed in Ref. [41]. The essential operation of this method is to replace the product of a full meson propagator, say $D(q)$, and the related interaction vertex function by the product of the corresponding free meson propagator $D_0(q)$ and a special current vertex functions. To explain how this method works, we define some composite operators:

$$J_I(z) = \bar{\psi}(z) I_{4 \times 4} \psi(z), \quad (\text{A18})$$

$$J^\nu(z) = \bar{\psi}(z) \gamma^\nu \psi(z), \quad (\text{A19})$$

$$J_3^\nu(z) = \bar{\psi}(z) \tau_3 \gamma^\nu \psi(z), \quad (\text{A20})$$

$$J_3(z) = \bar{\psi}(z) \tau_3 \psi(z), \quad (\text{A21})$$

where $\nu = 0, 1, 2, 3$. These composite operators are called current operators because their forms are similar to various (e.g., scalar, vector, isospin vector, and isospin scalar) currents. These current operators are then used to define a number of current vertex functions:

$$\langle J_I(z) \psi(z_1) \bar{\psi}(z_2) \rangle = \langle \bar{\psi}(z) I_{4 \times 4} \psi(z) \psi(z_1) \bar{\psi}(z_2) \rangle = - \int dz_3 dz_4 G(z_1 - z_3) \Upsilon_I(z, z_3, z_4) G(z_4 - z_2), \quad (\text{A22})$$

$$\langle J^\nu(z) \psi(z_1) \bar{\psi}(z_2) \rangle = \langle \bar{\psi}(z) \gamma^\nu \psi(z) \psi(z_1) \bar{\psi}(z_2) \rangle = - \int dz_3 dz_4 G(z_1 - z_3) \Gamma_{\gamma^\nu}(z, z_3, z_4) G(z_4 - z_2), \quad (\text{A23})$$

$$\langle J_3^\nu(z) \psi(z_1) \bar{\psi}(z_2) \rangle = \langle \bar{\psi}(z) \tau_3 \gamma^\nu \psi(z) \psi(z_1) \bar{\psi}(z_2) \rangle = - \int dz_3 dz_4 G(z_1 - z_3) \Theta_{\tau_3 \gamma^\nu}(z, z_3, z_4) G(z_4 - z_2), \quad (\text{A24})$$

$$\langle J_3(z) \psi(z_1) \bar{\psi}(z_2) \rangle = \langle \bar{\psi}(z) \tau_3 \psi(z) \psi(z_1) \bar{\psi}(z_2) \rangle = - \int dz_3 dz_4 G(z_1 - z_3) \Omega_{\tau_3}(z, z_3, z_4) G(z_4 - z_2). \quad (\text{A25})$$

Here, Υ_I , Γ_{γ^ν} , $\Theta_{\tau_3 \gamma^\nu}$, and Ω_{τ_3} are called current vertex

functions. Now we take the ωN coupling as an example

to demonstrate how to derive the relation satisfied by interaction and current vertex functions [41]. Making use of the invariance of Z under an infinitesimal variation of ω -meson field ω_μ , we derive an identity

$$g_\omega \langle \bar{\psi}(z) \gamma^\mu \psi(z) \rangle = [(\partial^2 + m_\omega^2) g^{\mu\nu} - \partial^\mu \partial^\nu] \omega_\nu(z) + J_\omega^\mu(z),$$

which is then cast into an equivalent form

$$g_\omega \langle \bar{\psi}(z) \gamma^\mu \psi(z) \rangle = [(\partial^2 + m_\omega^2) g^{\mu\nu} - \partial^\mu \partial^\nu] \frac{\delta W}{\delta J_\omega^\nu(z)} + J_\omega^\mu(z).$$

Carrying out functional derivatives with respect to $\bar{\eta}$ and η in order leads to

$$\begin{aligned} & \frac{\delta^2}{\delta \bar{\eta}(z_1) \delta \eta(z_2)} \langle \bar{\psi}(z) \gamma^\mu \psi(z) \rangle \\ &= \langle \bar{\psi}(z) \gamma^\mu \psi(z) \psi(z_1) \bar{\psi}(z_2) \rangle \\ &= g_\omega^{-1} [(\partial^2 + m_\omega^2) g^{\mu\nu} - \partial^\mu \partial^\nu] \frac{\delta^3 W}{\delta J_\omega^\nu(z) \delta \bar{\eta}(z_1) \delta \eta(z_2)}. \end{aligned}$$

Using Eq. (A23) and Eq. (A3), we obtain a relation

$$\begin{aligned} & \int dz_3 dz_4 G(z_1 - z_3) \Gamma_{\gamma^\mu}(z, z_3, z_4) G(z_4 - z_2) \\ &= \int dz_3 dz_4 dz_5 g_\omega^{-1} [(\partial^2 + m_\omega^2) g^{\mu\nu} - \partial^\mu \partial^\nu] \\ & \quad \times F_\nu^\rho(z - z_5) G(z_1 - z_3) \Gamma_\rho(z_5, z_3, z_4) G(z_4 - z_2). \end{aligned} \quad (\text{A26})$$

Under the condition of translational invariance, the current vertex function Γ_{γ^μ} is Fourier transformed as

$$\begin{aligned} \Gamma_{\gamma^\mu}(z_1, z, z_2) &\equiv \Gamma_{\gamma^\mu}(z_1 - z, z - z_2) \\ &= \int \frac{d^4 q d^4 k}{(2\pi)^8} e^{-i(k+q)(z_1-z)} \\ & \quad \times e^{-ik(z-z_2)} \Gamma_{\gamma^\mu}(q, k). \end{aligned}$$

Fourier transformation turns the relation (A26) into

$$\Gamma_{\gamma^\mu}(q, k) = g_\omega^{-1} F_{0\mu\nu}^{-1}(q) F_\nu^\rho(q) \Gamma_\rho(q, k). \quad (\text{A27})$$

It is more convenient to re-write this relation as

$$F^{\mu\nu}(q) \Gamma_\nu(q, k) = g_\omega F_0^{\mu\nu}(q) \Gamma_{\gamma_\nu}(q, k). \quad (\text{A28})$$

Based on the invariance of Z under arbitrary infinitesimal variations of σ , ρ_3^μ , and δ_3 fields, one could derive the following three exact identities

$$D(q) \Upsilon(q, k) = -g_\sigma D_0(q) \Upsilon_I(q, k), \quad (\text{A29})$$

$$V^{\mu\nu}(q) \Theta_\nu(q, k) = \frac{g_\rho}{2} V_0^{\mu\nu}(q) \Theta_{\tau_3 \gamma_\nu}(q, k), \quad (\text{A30})$$

$$C(q) \Omega(q, k) = -g_\delta C_0(q) \Omega_{\tau_3}(q, k). \quad (\text{A31})$$

Inserting the identities given by Eqs. (A28-A31) into the DS equation (A12), we get

$$\begin{aligned} G^{-1}(k) &= G_0^{-1}(k) - i g_\sigma^2 \int \frac{d^4 q}{(2\pi)^4} G(k+q) D_0(q) \Upsilon_I(q, k) \\ & \quad - i g_\omega^2 \int \frac{d^4 q}{(2\pi)^4} \gamma_\mu G(k+q) F_0^{\mu\nu}(q) \Gamma_{\gamma_\nu}(q, k) \\ & \quad - i \frac{g_\rho^2}{4} \int \frac{d^4 q}{(2\pi)^4} \tau_3 \gamma_\mu G(k+q) V_0^{\mu\nu}(q) \Theta_{\tau_3 \gamma_\nu}(q, k) \\ & \quad - i g_\delta^2 \int \frac{d^4 q}{(2\pi)^4} \tau_3 G(k+q) C_0(q) \Omega_{\tau_3}(q, k). \end{aligned} \quad (\text{A32})$$

The Feynman diagram of this DS equation is shown in Fig. 7. It should be emphasized that this DS equation is still exact, since it is derived from a number of identities. But this equation cannot be directly solved because the current vertex functions $\Upsilon_I(q, k)$, $\Gamma_{\gamma_\nu}(q, k)$, $\Theta_{\tau_3 \gamma_\nu}(q, k)$, and $\Omega_{\tau_3}(q, k)$ are not known. These functions have a complicated structure and cannot be expressed in terms of nucleon and meson propagators.

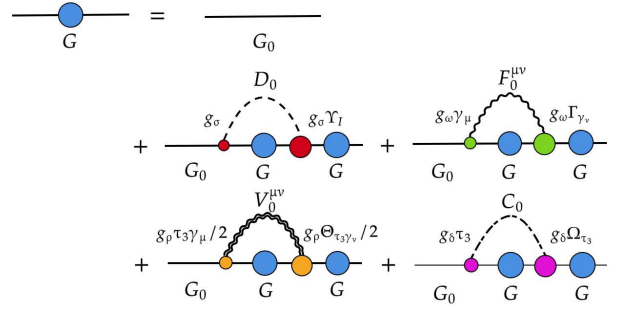


FIG. 7: A diagrammatic illustration of the exact DS equation of $G(k)$ given by Eq. (A32).

To tackle the above equation, we now introduce a crucial approximation. Let us focus on the expression $g_\sigma^2 \Upsilon_I(q, k)$. Before including vertex corrections, the parameter g_σ appearing in the Lagrangian density takes a certain bare value. It would be renormalized by vertex corrections to become $\tilde{g}_\sigma^2(q, k) = g_\sigma^2 \Upsilon_I(q, k)$. In principle, \tilde{g}_σ depend on energy and momentum. For calculational simplicity, we require \tilde{g}_σ to be a constant, under the assumption that it represents the mean value of $\tilde{g}_\sigma^2(q, k)$ obtained by averaging over all the allowed energies and momenta. This allows us to make the replacement

$$g_\sigma^2 \Upsilon_I(q, k) \rightarrow \tilde{g}_\sigma^2 I_{4 \times 4}. \quad (\text{A33})$$

The same manipulation can be applied to the other three coupling parameters, namely

$$g_\omega^2 \Gamma_{\gamma_\nu}(q, k) \rightarrow \tilde{g}_\omega^2 \gamma_\nu, \quad (\text{A34})$$

$$g_\rho^2 \Theta_{\tau_3 \gamma_\nu}(q, k) \rightarrow \tilde{g}_\rho^2 \tau_3 \gamma_\nu, \quad (\text{A35})$$

$$g_\delta^2 \Omega_{\tau_3}(q, k) \rightarrow \tilde{g}_\delta^2 \tau_3. \quad (\text{A36})$$

The renormalized coupling parameters \tilde{g}_σ , \tilde{g}_ω , \tilde{g}_ρ , and \tilde{g}_δ partially take into account the contributions of vertex corrections. Their realistic values are determined by comparing the theoretical results of ρ_{B0} , E_b , m_N^* , K , and E_s calculated at the saturation density to experimental data. The effects of vertex corrections are inherently present in the experimental values of observable quantities, and thus are naturally integrated into the simulated values of \tilde{g}_σ , \tilde{g}_ω , \tilde{g}_ρ , and \tilde{g}_δ . Purely for notational simplicity, we still use the symbols g_σ , g_ω , g_ρ , and g_δ to denote the renormalized coupling parameters. Formally, it is only

necessary to make the following replacement:

$$\Upsilon_I(q, k) \rightarrow I_{4 \times 4}, \quad (\text{A37})$$

$$\Gamma_{\gamma\nu}(q, k) \rightarrow \gamma_\nu, \quad (\text{A38})$$

$$\Theta_{\tau_3\gamma\nu}(q, k) \rightarrow \tau_3\gamma_\nu, \quad (\text{A39})$$

$$\Omega_{\tau_3}(q, k) \rightarrow \tau_3. \quad (\text{A40})$$

Then the DS equation (A32) is simplified to Eq. (4) presented in Sec. II.

-
- [1] N. K. Glendenning, *Compact Stars* (Springer, Berlin, 2000).
 - [2] J. M. Lattimer and M. Prakash, The physics of neutron stars, *Science* **304**, 536 (2004).
 - [3] J. M. Lattimer and M. Prakash, The equation of state of hot, dense matter and neutron stars, *Phys. Rep.* **621** 127 (2016).
 - [4] G. F. Burgio, H. J. Schulze, I. Vidaña, and J.-B. Wei, Neutron stars and the nuclear equation of state, *Prog. Part. Nucl. Phys.* **120**, 103879 (2021).
 - [5] J. D. Walecka, A theory of highly condensed matter, *Ann. Phys. (N.Y.)* **83**, 491 (1974).
 - [6] J. Boguta and A. R. Bodmer, Relativistic calculation of nuclear matter and the nuclear surface, *Nucl. Phys. A* **292**, 413 (1977).
 - [7] B. D. Serot, A relativistic nuclear field theory with π and ρ mesons, *Phys. Lett. B* **86**, 146 (1979).
 - [8] S. Kubis and M. Kutschera, Nuclear matter in relativistic mean field theory with isovector scalar meson, *Phys. Lett. B* **191**, 399 (1997).
 - [9] P.-G. Reinhard, The relativistic mean-field description of nuclei and nuclear dynamics, *Rep. Prog. Phys.* **52**, 439 (1989).
 - [10] M. Dutra *et al.*, Relativistic mean-field hadronic models under nuclear matter constraints, *Phys. Rev. C* **90**, 055203 (2014).
 - [11] M. Dutra *et al.*, Stellar properties and nuclear matter constraints, *Phys. Rev. C* **93**, 025806 (2016).
 - [12] G. A. Lalazissis, J. König, and P. Ring, New parametrization for the Lagrangian density of relativistic mean field theory, *Phys. Rev. C* **55**, 540 (1997).
 - [13] N. K. Glendenning and S. A. Moszkowski, Reconciliation of neutron-star masses and binding of the Λ in hypernuclei, *Phys. Rev. Lett.* **67**, 2414 (1991).
 - [14] Y. Sugahara and H. Toki, Relativistic mean-field theory for unstable nuclei with non-linear σ and ω terms, *Nucl. Phys. A* **579**, 557 (1994).
 - [15] C. J. Horowitz and J. Piekarewicz, Neutron star structure and the neutron radius of ^{208}Pb , *Phys. Rev. Lett.* **86**, 5647 (2001).
 - [16] B. G. Todd-Rutel and J. Piekarewicz, Neutron-rich nuclei and neutron stars: A new accurately calibrated interaction for the study of neutron-rich matter, *Phys. Rev. Lett.* **95**, 122501 (2005).
 - [17] F. J. Fattoyev, C. J. Horowitz, J. Piekarewicz, and B. Reed, GW190814: Impact of a 2.6 solar mass neutron star on the nucleonic equations of state, *Phys. Rev. C* **102**, 065805 (2020).
 - [18] S. Typel and H. H. Wolter, Relativistic mean field calculations with density-dependent meson-nucleon coupling, *Nucl. Phys. A* **656**, 331 (1999).
 - [19] G. A. Lalazissis, T. Nikšić, D. Vretenar, and P. Ring, New relativistic mean-field interaction with density-dependent meson-nucleon couplings, *Phys. Rev. C* **71**, 024312 (2005).
 - [20] S. Typel, G. Röpke, T. Klähn, D. Blaschke, and H. H. Wolter, Composition and thermodynamics of nuclear matter with light clusters, *Phys. Rev. C* **81**, 015803 (2010).
 - [21] S. Typel and D. A. Terrero, Parametrisations of relativistic energy density functionals with tensor couplings, *Eur. Phys. J. A* **56**, 160 (2020).
 - [22] A. Taninah, S. E. Agbemava, A. V. Afanasjev, and P. Ring, Parametric correlations in energy density functionals, *Phys. Lett. B* **800**, 135065 (2020).
 - [23] A. L. Fetter and J. D. Walecka, *Quantum Theory of Many-Particle Systems* (McGraw-Hill, New York, 2003).
 - [24] E. Epelbaum, H. W. Hammer, and Ulf-G. Meissner, Modern theory of nuclear forces, *Rev. Mod. Phys.* **81**, 1773 (2009).
 - [25] R. Machleidt and D. R. Entem, Chiral effective field theory and nuclear forces, *Phys. Rep.* **503**, 1 (2011).
 - [26] J. Carlson *et al.*, Quantum Monte Carlo methods for nuclear physics, *Rev. Mod. Phys.* **87**, 1067 (2015).
 - [27] I. Tews, J. Carlson, S. Gandolfi, and S. Reddy, Constraining the speed of sound inside neutron stars with chiral effective field theory interactions and observations, *Astrophys. J.* **860**, 149 (2018).
 - [28] S. Huth, P. T. H. Pang, I. Tews, T. Dietrich, A. Le Fèvre, A. Schwenk, W. Trautmann, K. Agarwal, M. Bulla, M. W. Coughlin, and C. Van Den Broeck, Constraining neutron-star matter with microscopic and macroscopic collisions, *Nature (London)* **606**, 276 (2022).
 - [29] B. P. Abbott *et al.*, GW170817: observation of gravitational waves from a binary neutron star inspiral, *Phys. Rev. Lett.* **119**, 161101 (2017).
 - [30] B. P. Abbott *et al.*, GW170817: measurements of neutron star radii and equation of state, *Phys. Rev. Lett.* **121**, 161101 (2018).
 - [31] M. C. Miller, F. K. Lamb, A. J. Dittmann, S. Bogdanov, Z. Arzoumanian, K. C. Gendreau, S. Guillot, A. K. Harding, W. C. G. Ho, J. M. Lattimer, R. M. Ludlam, S. Mahmoodifar, S. M. Morsink, P. S. Ray, T. E. Strohmayer, K. S. Wood, T. Enoto, R. Foster, T. Okajima, G. Prigozhin,

- and Y. Soong, PSR J0030+0451 mass and radius from NICER data and implications for the properties of neutron star matter, *Astrophys. J. Lett.* **887**, L24 (2019).
- [32] T. E. Riley, A. L. Watts, S. Bogdanov, P. S. Ray, R. M. Ludlam, S. Guillot, Z. Arzoumanian, C. L. Baker, A. V. Bilous, D. Chakrabarty, K. C. Gendreau, A. K. Harding, W. C. G. Ho, J. M. Lattimer, S. M. Morsink, and T. E. Strohmayer, A NICER view of PSR J0030+0451: Millisecond pulsar parameter estimation, *Astrophys. J. Lett.* **887**, L21 (2019).
- [33] M. C. Miller, F. K. Lamb, A. J. Dittmann, S. Bogdanov, Z. Arzoumanian, K. C. Gendreau, S. Guillot, W. C. G. Ho, J. M. Lattimer, M. Loewenstein, S. M. Morsink, P. S. Ray, M. T. Wolff, C. L. Baker, T. Cazeau, S. Manthripragada, C. B. Markwardt, T. Okajima, S. Pollard, I. Cognard *et al.*, The radius of PSR J0740+6620 from NICER and XMM-Newton data, *Astrophys. J. Lett.* **918**, L28 (2021).
- [34] T. E. Riley, A. L. Watts, P. S. Ray, S. Bogdanov, S. Guillot, S. M. Morsink, A. V. Bilous, Z. Arzoumanian, D. Choudhury, J. S. Deneva, K. C. Gendreau, A. K. Harding, W. C. G. Ho, J. M. Lattimer, M. Loewenstein, R. M. Ludlam, C. B. Markwardt, T. Okajima, C. Prescod-Weinstein, R. A. Remillard *et al.*, A NICER view of the massive pulsar PSR J0740+6620 informed by radio timing and XMM-Newton spectroscopy, *Astrophys. J. Lett.* **918**, L27 (2021).
- [35] P. Demorest, T. Pennucci, S. M. Ransom, M. S. E. Roberts, and J. W. T. Hessels, A two-solar-mass neutron star measured using Shapiro delay, *Nature (London)* **467**, 1081 (2010).
- [36] J. Antoniadis, P. C. C. Freire, N. Wex, T. M. Tauris, R. S. Lynch, M. H. van Kerkwijk, M. Kramer, C. Bassa, V. S. Dhillon, T. Driebe, J. W. T. Hessels, V. M. Kaspi, V. I. Kondratiev, N. Langer, T. R. Marsh, M. A. McLaughlin, T. T. Pennucci, S. M. Ransom, I. H. Stairs, J. van Leeuwen *et al.*, A massive pulsar in a compact relativistic binary, *Science* **340**, 1233232 (2013).
- [37] H. T. Cromartie, E. Fonseca, S. M. Ransom, P. B. Demorest, Z. Arzoumanian, H. Blumer, P. R. Brook, M. E. DeCesar, T. Dolch, J. A. Ellis, R. D. Ferdman, E. C. Ferrara, N. Garver-Daniels, P. A. Gentile, M. L. Jones, M. T. Lam, D. R. Lorimer, R. S. Lynch, M. A. McLaughlin, C. Ng *et al.*, Relativistic Shapiro delay measurements of an extremely massive millisecond pulsar, *Nat. Astron.* **4**, 72 (2019).
- [38] R. W. Romani, D. Kandel, A. V. Filippenko, T. G. Brink, and W. Zheng, PSR J0952-0607: The fastest and heaviest known galactic neutron star, *Astrophys. J. Lett.* **934**, L17 (2022).
- [39] C. Itzykson and J.-B. Zuber, *Quantum Field Theory* (McGraw-Hill, New York, 1980).
- [40] C. D. Roberts and S. M. Schmidt, Dyson-Schwinger equations: density, temperature and continuum strong QCD, *Prog. Part. Nucl. Phys.* **45**, S1-S103 (2000).
- [41] G.-Z. Liu, Z.-K. Yang, X.-Y. Pan, and J.-R. Wang, Towards exact solutions for the superconducting T_c induced by electron-phonon interaction, *Phys. Rev. B* **103**, 094501 (2021).
- [42] X.-Y. Pan, Z.-K. Yang, X. Li, and G.-Z. Liu, Nonperturbative Dyson-Schwinger equation approach to strongly interacting Dirac fermion systems, *Phys. Rev. B* **104**, 085141 (2021).
- [43] J. Bardeen, L. N. Cooper, and J. R. Schrieffer, Theory of Superconductivity, *Phys. Rev.* **108**, 1175 (1957).
- [44] D. J. Scalapino, *The electron-phonon interaction and strong-coupling superconductivity*, in *Superconductivity*, edited by R. D. Parks (Marcel Dekker, New York, 1969).
- [45] J. M. Luttinger and J. C. Ward, Ground-state energy of a many-fermion system.II, *Phys. Rev.* **118**, 1417 (1960).
- [46] D. Foreman-Mackey, D. W. Hogg, D. Lang, and J. Goodman, emcee: The MCMC Hammer. *Publ. Astron. Soc. Pac.* **125**, 306 (2013).
- [47] R. C. Tolman, Static solutions of Einstein's field equations for spheres of fluid, *Phys. Rev.* **55**, 364 (1939).
- [48] J. R. Oppenheimer and G. M. Volkoff, On massive neutron cores, *Phys. Rev.* **55**, 374 (1939).
- [49] T. Hinderer, Tidal Love numbers of neutron stars, *Astrophys. J.* **677**, 1216 (2008).
- [50] S. Postnikov, M. Prakash, and J. M. Lattimer, Tidal Love numbers of neutron and self-bound quark stars, *Phys. Rev. D* **82**, 024016 (2010).
- [51] X. Wu, S. Bao, H. Shen, and R. Xu, Effect of the symmetry energy on the secondary component of GW190814 as a neutron star, *Phys. Rev. C* **104**, 015802 (2021).
- [52] E. Annala, T. Gorda, A. Kurkela, and A. Vuorinen, Gravitational-wave constraints on the neutron-star-matter equation of state, *Phys. Rev. Lett.* **120**, 172703 (2018).
- [53] R. Abbott, T. D. Abbott, S. Abraham, F. Acernese, K. Ackley, C. Adams, R. X. Adhikari, V. B. Adya, C. Affeldt, M. Agathos, K. Agatsuma, N. Aggarwal, O. D. Aguiar, A. Aich, L. Aiello, A. Ain, P. Ajith, S. Akcay, G. Allen, A. Allocca *et al.*, GW190814: Gravitational waves from the coalescence of a 23 solar mass black hole with a 2.6 solar mass compact object, *Astrophys. J. Lett.* **896**, L44 (2020).
- [54] M. Prakash, I. Bombaci, M. Prakash, P. J. Ellis, J. M. Lattimer, and R. Knorren, Composition and structure of protoneutron stars, *Phys. Rep.* **280**, 1 (1997).
- [55] L. Baiotti and L. Rezzolla, Binary neutron star mergers: a review of Einstein's richest laboratory, *Rep. Prog. Phys.* **80**, 096901 (2017).
- [56] J. J. Li, A. Sedrakian, and F. Weber, Competition between delta isobars and hyperons and properties of compact stars, *Phys. Lett. B* **783**, 234 (2018).
- [57] A. Sedrakian, F. Weber, and J. J. Li, Confronting GW190814 with hyperonization in dense matter and hypernuclear compact stars, *Phys. Rev. D* **102**, 041301 (2020).
- [58] A. Sedrakian and J. W. Clark, Superfluidity in nuclear systems and neutron stars, *Eur. Phys. J. A* **55**, 167 (2019).
- [59] D. Page, J. M. Lattimer, M. Prakash, and A. W. Steiner, Stellar Superfluids, in *Novel Superfluids*, edited by K.-H. Bennemann and J. B. Ketterson (Oxford, 2014).
- [60] E. Annala, T. Gorda, A. Kurkela, J. Nättilä, and A. Vuorinen, A. Evidence for quark-matter cores in massive neutron stars, *Nat. Phys.* **16**, 907 (2020).
- [61] E. Annala, T. Gorda, J. Hirvonen, O. Komoltsev, A. Kurkela, J. Nättilä, and A. Vuorinen, Strongly interacting matter exhibits deconfined behavior in massive neutron stars, *Nat. Commun.* **14**, 8451 (2023).